Combined effects of elevated pCO_2 and nitrogen limitation on bloom-forming dinoflagellate species

Produced at the Alfred Wegener Institute for Marine and Polar Research
Bremerhaven, Section Marine BioGeoScience

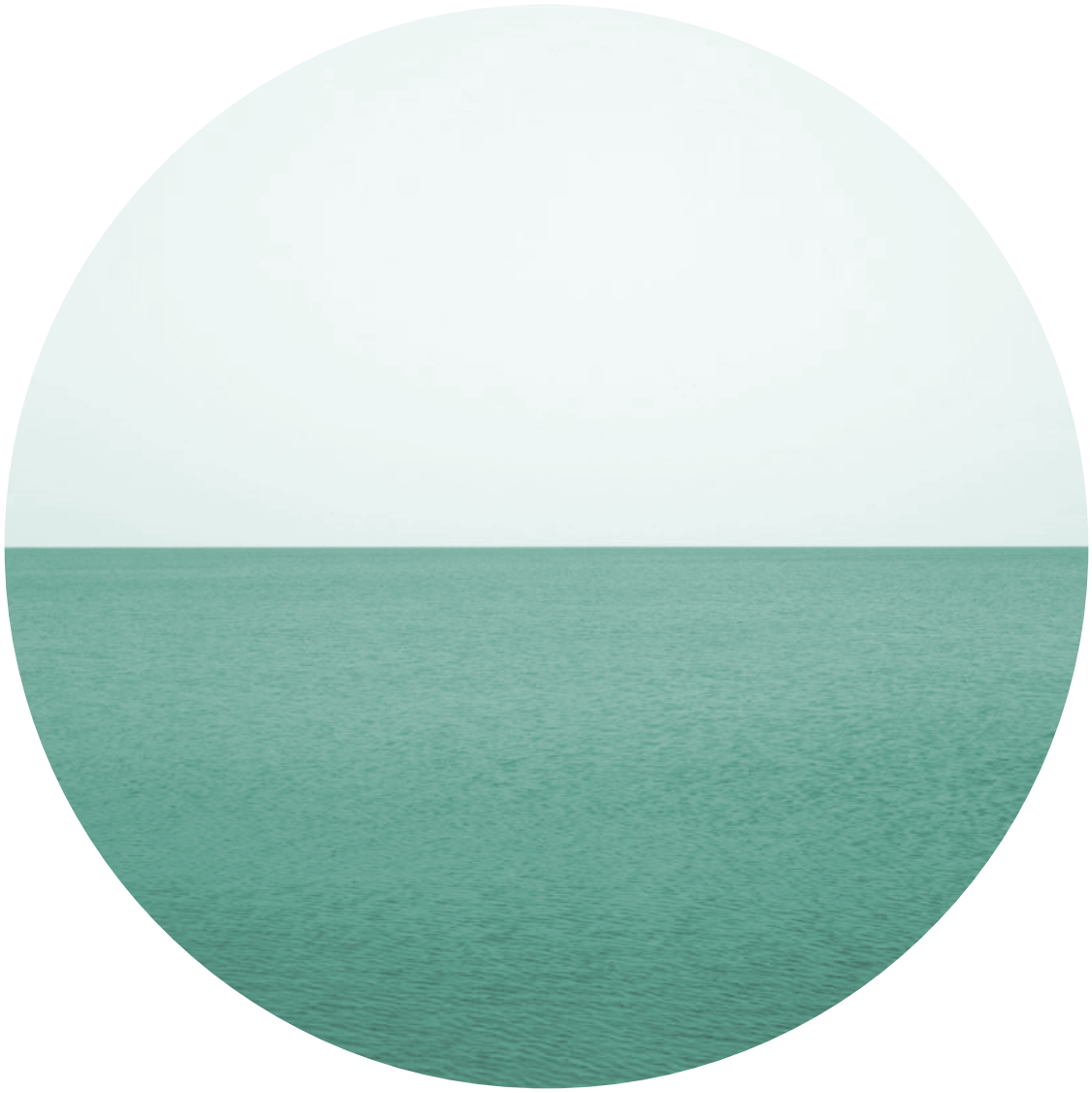

By Karen Brandenburg
Utrecht University
Faculty of Geosciences
Department of Earth Sciences
March 2014

Supervised by
Tim Eberlein (Alfred Wegener Institute)
Dr. Björn Rost (Alfred Wegener Institute)
Dr. Dedmer B. van de Waal (NIOO-KNAW)
Dr. Francesca Sangiorgi (Utrecht University)

Universiteit Utrecht

Table of contents

List of figures and tables

List of abbreviations

A. tamarense	*Alexandrium tamarense*
(aq)	Aqueous
C	Carbon
CA	Carbonic anhydrase
$CaCO_3$	Calcium carbonate
CCM	Carbon concentrating mechanism
Chl *a*	Chlorophyll *a*
CO_2	Carbon dioxide
CO_3^{2-}	Carbonate ion
DIC	Dissolved inorganic carbon
$\delta^{13}C_{DIC}$	Isotopic fractionation of dissolved inorganic carbon
$\delta^{13}C_{POC}$	Isotopic fractionation of particulate organic carbon
ε_p	Isotopic fractionation during particulate organic carbon formation
(g)	Gaseous
HAB	Harmful algal bloom
H_2CO_3	Carbonic acid
HCO_3^-	Bicarbonate ion
K_0, K_1, K_2	Equilibrium constants
$K_{1/2}$	Substrate concentration at which the reaction rate is half saturated (on a cellular level)
K_N	Nitrate concentration at which the reaction rate of N-transporter enzymes is half saturated

m	Mortality rate
N	Nitrogen
NUE	Nitrate use efficiency
NPP	Net primary production
pCO_2	Atmospheric partial pressure of CO_2
$pH_{(NBS)}$	pH according to the national bureau of standards
PIC	Particulate inorganic carbon
POC	Particulate organic carbon
PON	Particulate organic nitrogen
PST	Paralytic shellfish poisoning toxins
Q_{min}	Internal nutrient concentration
R*	Minimal resource requirement of a species
S	Salinity
SD	Standard deviation
SST	Sea surface temperature
S. trochoidea	*Scrippsiella trochoidea*
RubisCO	Ribulose 1,5-bisphosphate carboxylase/oxygenase
T	Temperature
TA	Total alkalinity
TEP	Transparent exopolymer particles
TPC	Total particulate carbon
µatm	Micro-atmosphere (unit of pCO_2)
V_m	Maximum uptake rate of a particular substrate
V_{maxN}	Maximum uptake rate of nitrate

Summary

Atmospheric CO_2 levels are rising rapidly due to anthropogenic influences. About 25-30% of the CO_2 released due to anthropogenic activities over the last decades has already entered the surface oceans, causing changes in the aquatic carbonate chemistry, a phenomenon also known as "ocean acidification". Ocean acidification will have a huge impact on the different phytoplankton species living in the surface waters, as a lowering in the pH can negatively affect calcification and CO_2 elevation can promote photosynthesis. Dinoflagellates are expected to be most sensitive to changes in CO_2 availability due to their possession of form II RubisCO, which exhibits the lowest affinities for its substrate CO_2 among all eukaryotic phytoplankton. CO_2 also acts as a greenhouse gas, which will cause future atmospheric and surface ocean temperatures to rise, and thus will enhance stratification. Under enhanced upper ocean stratification, upwelling will decrease and the nutrient resupply from below will become severely reduced. Effects of ocean acidification on the eco-physiology of phytoplankton have proven to be strongly modulated in combination with other environmental stressors. Decreased nitrate availability could be especially important since N is the second most required nutrient for phytoplankton and the assimilation of carbon and nitrogen are closely coupled. In view of elevated CO_2 concentrations in a nitrate-depleted, future ocean, changes in C and N assimilation could strongly interact and lead to major eco-physiological shifts of phytoplankton. For instance, the excess of energy from a down-regulation of the CCM could potentially be reallocated into N assimilation and thereby alter the nitrate use efficiency. To assess the effects of elevated pCO_2 under nitrogen limitation we investigated the marine dinoflagellate species *Scrippsiella trochoidea* in newly developed continuous culture mixing systems. Cultures were grown under three different CO_2 treatments (300, 600 and 800 µatm) with a starting nitrate concentration of 8 µmol l^{-1}. The elemental composition of *S. trochoidea* did not show significant variations in response to different CO_2 levels, but a change in resource use efficiency was observed. In the 800 CO_2 treatment, the R* for nitrate decreased, which was in contrast with our expectations, since under elevated pCO_2 more energy could be re-allocated towards N assimilation. One explanation for the observed response is that the lower pH in this treatment could have limited nutrient uptake. Shifts in resource use efficiency under future ocean conditions could eventually be the trigger for shifts in dominance of species with likely consequences also for higher trophic levels. Strikingly, PON and Chl *a* content per cell remained unaltered when compared to N-replete cultures, but cell size and POC content per cell increased, which lead to the observed a 2.5 fold increase in C/N ratios in all CO_2 treatments. Since PON and Chl *a* remained unaltered, the rate of photosynthesis could be largely unaffected, although production rates did decrease, and carbon fixation served as a major sink for the excess of energy within the cell, thus explaining the increases in cell size and POC content. The changes in elemental composition under N-limitation can have huge ecological consequences, for instance on the food web. This study indicates that the eco-physiology of dinoflagellates will be strongly affected by future ocean conditions. It is therefore of imperative importance to conduct further phytoplankton experiments using this multiple stressor approach in order to increase our knowledge of phytoplankton responses to future climate scenarios.

Introduction

Earth's climate

On geological time scales, the Earth's climate has undergone major changes, with processes such as Earth-orbital variations and tectonic activity being mainly hold responsible (Ruddiman, 2008). One of the most important processes currently influencing the climate system is anthropogenic forcing. Human agricultural and industrial activities, for instance, emit CO_2 to the atmosphere at a rate which has no known precedent in the past (Jansen et al., 2007). It is generally argued that the atmospheric CO_2 levels have remained below 300 µatm over the past 10 million years, with fluctuations between 180-300 µatm during the glacial-interglacial cycles over the last 400,000 years (**fig. 1**; Pearson & Palmer, 2000; Lüthi et al., 2008; Petit et al., 1999). However, due to anthropogenic activity, atmospheric partial pressure of CO_2 (pCO_2) has already reached about 390 µatm at present-day and from model calculations pCO_2 is expected to rise up to 1,000 µatm by the end of this century (Solomon et al., 2007; Forster et al., 2007; Houghton et al., 2001).

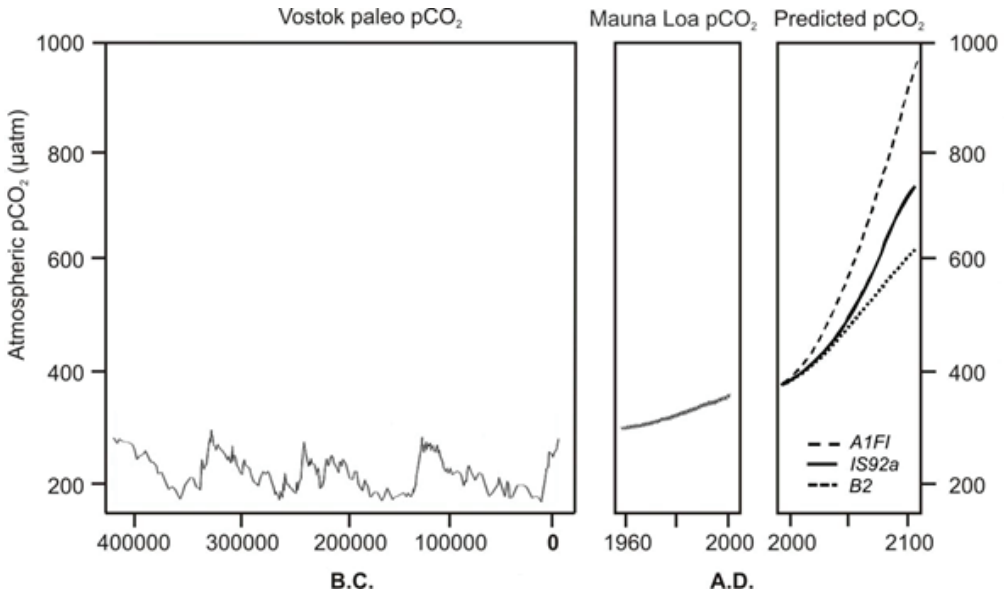

Figure 1. Atmospheric partial pressure of CO_2 (pCO_2) over time.

The Vostok paleo-record of pCO_2 shows the fluctuations over the last 420,000 years, the oscillations represent the glacial-interglacial cycles (Petit et al., 1999). The Mauna Loa record shows fluctuations of pCO_2 from 1960 until 2000 (Keeling et al., 2005). Three possible scenarios are predicted for future pCO_2: B2 represents the sustainability scenario, A1FI the worst case scenario and IS92a the business as usual scenario (Solomon et al., 2007).

Biological carbon pumps

The oceans are the largest active carbon reservoir on Earth, with a contemporary carbon exchange between the atmosphere and the ocean amounting to approximately 90 Gt C y^{-1} in both directions (Suttle, 2005; Ruddiman, 2008). The CO_2 transfer from atmosphere to ocean is driven by the solubility of CO_2

according to Henry's Law. At high latitudes, where temperatures is decreasing, more CO_2 can be taken up by the ocean (IPCC, 2007) and seawater density is increasing. Also, during the formation of sea ice, salinity of the surface water rises. Furthermore, sea ice formation causes an increase in the water density and the surface water will sink deeper into the ocean interior. Consequently, there is a vertical gradient with increasingly dissolved inorganic carbon (DIC) concentrations from the surface waters to the deeper ocean. However, this explains only 25 % of the current vertical DIC gradient. The remaining 75% of the vertical DIC gradient can be explained by the phytoplankton-driven "biological pumps" (Sarmiento et al., 1995). Through biological processes, such as photosynthesis and calcification, phytoplankton use DIC in the surface layers to form organic compounds (particulate organic carbon; POC) and calcite shells (particulate inorganic carbon; PIC). These compounds sink more rapidly to the ocean interior compared to DIC, and partially remineralise and dissolve during sedimentation (Jiao et al., 2010). In fact, of the organic material that sinks through the water column, only 0.5 to 2% eventually reaches the ocean floor, depending on water depth and variations in levels of primary production (Smith et al., 2008). Without the biological carbon pumps, model calculations indicate that atmospheric CO_2 concentrations would be twice as high as that of today (Maier-Reimer et al., 1996), which illustrates the general importance of the pumps for the uptake capacity of the oceans as well as their potential role in climate regulation.

Direct CO_2 effects on the ocean

The rising CO_2 concentrations in the atmosphere have already proven to directly affect the carbonate chemistry in the surface ocean (Feely et al., 2008; Cai et al., 2011). This can be attributed to the ability of CO_2 not only to dissolve in water, via equilibration of CO_2 (g) and CO_2 (aq), but also to further react with water molecules. Hence, dissolved CO_2 and water molecules form carbonic acid (H_2CO_3), which is an unstable compound and quickly dissociates into bicarbonate (HCO_3^-) and carbonate ions (CO_3^{2-}), according to the first (K_1) and second (K_2) dissociation constants of H_2CO_3 (**fig. 2**). During these reaction steps, protons (H^+) are released (Zeebe & Wolf-Gladrow, 2001). An increase in oceanic CO_2 uptake will thus not only increase the DIC concentration in seawater, but will also result in a drop in pH. This phenomenon is often referred to as "ocean acidification" (Caldeira & Wickett, 2003; Rost et al., 2008; Doney et al., 2009). As

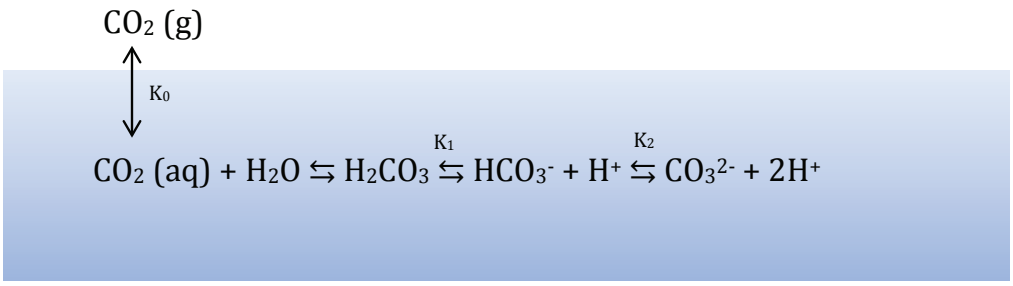

Figure 2. Schematic overview of the carbonate species in the surface ocean

Schematic overview of the relation between the carbonate species in the surface ocean and atmosphere, in equilibrium according to K_0, K_1 and K_2, where K_0 represents the solubility of CO_2 in seawater according to Henry's Law, dependent on salinity, pressure and temperature.

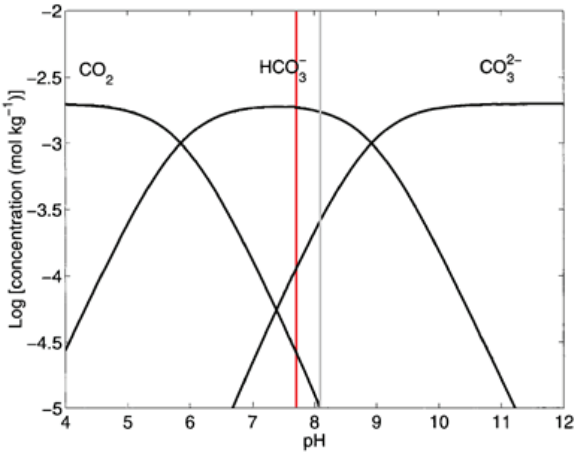

Figure 3. The Bjerrum plot, carbon speciation over a pH range

The Bjerrum plot at a temperature of 25°C and a salinity of 35‰ (Zeebe & Wolf-Gladrow, 2001). Concentrations of the inorganic dissolved carbon species are given in mol kg^{-1} at different pH values. The grey line indicates the current oceanic pH and the red line the expected pH value over 100 years (ocean acidification). Even though pH is plotted on the x-axis, pH is not the forcing parameter of the carbonate system.

a consequence of the chemical reactions of CO_2 with water (**fig. 2**), the oceans can hold up to a thousand times more CO_2 than either N_2 or O_2 (Garrison, 2007). The concentrations of the different DIC species vary, however.

From the CO_2 emitted via anthropogenic activity, 25-30% already entered the surface ocean over the last decades, causing changes in the marine carbonate chemistry (Wolf-Gladrow et al., 1999; Ruddiman, 2008). Higher pCO_2 already resulted in a drop in surface ocean pH from 8.21 to 8.10 between 1750 and 1994 (Raven et al., 2005). pH is expected to drop even further in the future with increasing pCO_2. At current atmospheric CO_2 levels and a pH of around 8.1 (**fig. 3**, grey line), by far the largest portion of DIC in the ocean is composed of HCO_3^- (~90%), followed by CO_3^{2-} (9%) and CO_2 (<1%; **fig. 3**; Zeebe & Wolf-Gladrow, 2001). By the year 2100, atmospheric CO_2 levels are expected to have tripled compared to preindustrial values. Concomitantly, CO_2 (aq) and HCO_3^- will increase by more than 300% and 10%, respectively, while CO_3^{2-} ions and pH will drop by 70% and 0.4 units, respectively (**fig. 3**, red line) (Wolf-Gladrow et al., 1999).

Because of this enormous CO_2-uptake capacity of the oceans, they are often referred to as a CO_2-buffer and can contain as much as 60 times more inorganic carbon than the atmosphere (Garrison, 2007). However the carbonate system can be somewhat counter-intuitive as a doubling of the atmospheric CO_2 concentration only leads to an increase in DIC of 10%. This effect is described by the Revelle factor (RF_0), a quantitative expression for CO_2-buffering, which describes the ratio between the relative change in CO_2 and the relative change in DIC (Zeebe & Wolf-Gladrow, 2001):

$$RF_0\ (T, S, pCO_2) = \frac{\Delta[CO_2]/\Delta[CO_2]}{\Delta[DIC]/\Delta[DIC]}$$

where T and S represent temperature and salinity, respectively. Thus when atmospheric CO_2 concentrations increase, it will result in a relatively small change in DIC. At the same time, however, it will affect the ocean's uptake capacity for CO_2 is reduced since the Revelle factor itself is dependent on pCO_2 (Sabine et al., 2004).

Besides salinity, temperature and pressure, the carbon speciation and thereby the buffer capacity of the oceans is also influenced by alkalinity. The total buffer capacity of the oceans can therefore be expressed as total alkalinity (TA). Next to the different carbon species, which can function as a buffer, seawater also contains many dissolved anions, which, in turn, can take up protons and act as a buffer. Among the various definitions of TA (Dickson, 1981), the explicitly conservative is defined as a sum of the major ions in seawater and acid-base species (Wolf-Gladrow et al., 2007):

$$TA = [Na^+] + 2[Mg^{2+}] + 2[Ca^{2+}] + [K^+] \ldots$$
$$-[Cl^-] - [Br^-] - [NO_3^-] - [PO_{4(T)}] - [SO_{4(T)}] \ldots$$

Changes in temperature, pressure and CO_2 concentrations do not affect alkalinity, as the charge balance remains unaffected. Biological processes however can cause changes in alkalinity. Calcifying species can significantly decrease alkalinity by taking up Ca^{2+} to form calcite structures ($CaCO_3$), which can result in a lowering of pH. In addition, uptake of nutrients can be responsible for alterations in TA. However, organisms can compensate for this uptake by exchanging non-nutrients, such as Cl^- and H^+ with their environment.

Indirect CO_2 effects on the ocean

Besides the direct effects of elevated CO_2 levels on the ocean (e.g. changes in carbonate chemistry), elevated CO_2 levels also influence the marine environment in an indirect matter, as CO_2 is the most important greenhouse gas after water vapor and therefore a major driver of global warming (Crosson, 2008). Over geological timescales, there is a strong correlation between atmospheric CO_2 concentrations and global average temperatures (Doney & Schimel, 2007). Since the late 1800s, increasing CO_2 concentrations have caused an increase in average global temperatures of 0.7 °C (Jones & Mann, 2004). By the end of this century, temperatures are expected to rise between 2-6 °C, with changes being more pronounced at high latitudes (IPCC, 2007). Rising atmospheric temperatures will also increase the sea surface temperature (SST; **fig. 4**). This, in turn, will cause a difference in densities between the upper water bodies, thus enhancing the stratification of the water column as well as a

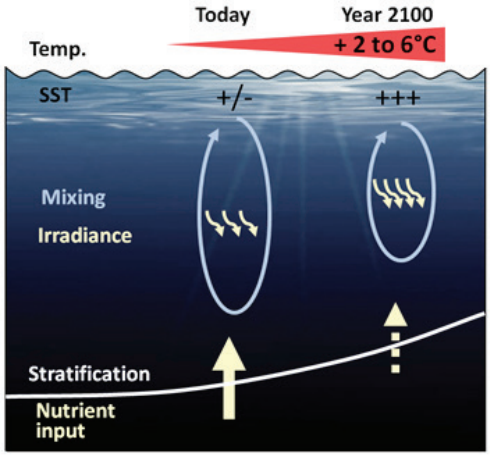

Figure 4. Indirect CO_2 effects on the future ocean

Differences in sea surface temperature (SST), stratification, mixing depth, irradiance and nutrient input of today and in the year 2100, as a consequence of global warming (Rost et al., 2008).

shoaling of the upper mixed layer (Garrison, 2007). Under these conditions, the nutrient resupply from below will be severely reduced which will result in more oligotrophic regions in the subtropics (Behrenfield et al., 2006). Due to the shoaling, irradiance will be higher in the upper mixed layer (**fig. 4**; Sarmiento et al., 2004). The marine ecosystem is thus undergoing major changes on a short timescale. Especially primary producers might be strongly affected, as they thrive in the euphotic zone where changes will be most pronounced (Rost et al., 2008).

Marine phytoplankton groups

On average, phytoplankton accounts for almost half of all primary productivity on Earth, which is 49.3 Gt C yr^{-1} (Field et al., 1998; Wilhelm & Suttle, 1999). As it forms the basis of nearly every aquatic food web and plays an active role in biogeochemical cycles (Falkowski, 1994), this emphasizes the importance of understanding the impact of rising CO_2 levels on phytoplankton and hence its feedback on the biogeochemical cycles. Different phytoplankton species have varying ecological roles and contribute differentially to the net primary production (NPP) of the oceans. Among phytoplankton, there is one main prokaryotic group, namely cyanobacteria, and there are three main eukaryotic groups, namely coccolithophores, diatoms and dinoflagellates (Falkowski et al., 2004). Cyanobacteria are in numbers the largest phytoplankton group (Sumich & Morrissey, 2004). Some are diazotrophs and able to fix nitrogen gas (N_2), therefore providing a major source of new nitrogen to the water column, which becomes available for biomass production of other phytoplankton species (Karl et al., 1997; Capone et al., 2005). Coccolithophores have a cell wall covered with calcite disks, so-called coccoliths. Through the production and export of $CaCO_3$, they cause strong gradients in DIC and in TA relative to other phytoplankton groups and thus play a significant role in the global carbon cycle (Falkowski & Knoll, 2007; Garrison, 2007). Diatoms are the most productive phytoplankton species and contribute up to 50 % to the oceans primary production (Nelson et al., 1995). The last and often neglected group of phytoplankton are the dinoflagellates. They form a diverse group with complex interactions in the food web as some species are mixotrophic and some species are known to produce toxins (Schnepf & Elbrächter, 1992; Smayda, 1997). Dinoflagellates are known to produce cysts, which can either be vegetative, produced in the motile life stage, or resting cysts, that lay dormant and remain viable for up to a 100 years in the sediment (Hoppenrath & Saldarriagga, 2012). Some dinoflagellates can produce resting cysts with calcite walls, such as Scrippsiella spp. (Olli & Anderson 2002; Wang et al., 2007). Dinoflagellates can thrive in all aquatic environments and some are the photosynthetic endosymbionts of corals (Hoegh-Guldberg et al., 2007). Additionally some dinoflagellates are well known for causing harmful algal blooms (HABs), phenomena that seem to have become more frequent over the past decades due to eutrophication and climate change (Anderson et al., 2002; Glibert et al., 2005). HABs are often also called "red tides" due to the discoloration of the water these blooms cause at times. Some bloom-forming species, like the genus *Alexandrium*, produce paralytic shellfish poisoning toxins (PST), which can accumulate in the food chain and have large ecological and economic consequences (Smayda, 1997; Anderson et al., 2002). HABs have been shown to be particularly promoted by enhanced nutrient loads

and temperature. The impacts of ocean acidification on growth and toxicity of HABs, however, is not well understood.

Carbon acquisition in phytoplankton

In order to predict the effects of rising pCO_2 on phytoplankton, an understanding of the photosynthesis and the subsequent downstream processes is required. Photosynthesis involves a chain of reactions that start with capturing light energy, transferring it into the energy-maintaining compounds NADPH and ATP, and subsequently use these compounds to fix CO_2 in the Calvin cycle (Falkowsky & Raven, 2007). As a result photosynthesis and downstream processes are primarily light-dependent, but are also influenced by CO_2 availability (Rost et al., 2008). In the cell, CO_2 is fixed by the carboxylating enzyme, ribulose-1,5-bisphosphate carboxylase/oxygenase (RubisCO), which has a half-saturation constant (K_m) for its substrate CO_2 ranging from 20 to 180 µmol kg^{-1} (Badger et al., 1998). However typical seawater contains CO_2 concentrations within a range of 10-25 µmol kg^{-1}, therefore making RubisCO insufficient to ensure effective carboxylation when cells rely on diffusive CO_2-uptake only. Moreover, at present day O_2 levels, RubisCO can be prone to photorespiration.

The inherent low affinity of RubisCO and the sensitivity towards O_2 can be overcome by algae through the operation of so-called carbon concentrating mechanisms (CCM). It ultimately functions to enhance the CO_2 concentration in the vicinity of RubisCO (Badger et al., 1998), thereby allowing saturation in photosynthesis already at very low DIC concentrations in the water. CCMs can comprise active uptake of CO_2 and/or HCO_3^-, the use of carbonic anhydrase (CA) activity to accelerate the interconversion of CO_2 and HCO_3^-, and minimization of CO_2 efflux from the cell (**fig. 5**; Giordano et al., 2005). Efficiency to reach saturation, operational costs and the ability of regulation of the CCM differ among phytoplankton species and define the sensitivity of a species towards changes in pCO_2 (Raven & Beardall 2003; Rost et al., 2008). Species with an absent or inefficient CCM that mostly rely on diffusive CO_2 uptake alone will benefit from future CO_2 levels in a direct manner (Colman et al., 2004). In contrast, species with highly efficient CCMs, which are saturated at present-day CO_2 levels, can nonetheless benefit in a future "high CO_2" ocean by down-regulation of their CCMs and subsequent allocation of energy and resources (Rost et al., 2008). Different phytoplankton species can thus show a variety of responses to future CO_2 levels as the applied mode of CCM is proven to be species-specific (Rost et al., 2003; Tortell & Morel, 2002).

Eco-physiology of dinoflagellates

Dinoflagellates are expected to be most sensitive to changes in CO_2 availability due to their possession of form II RubisCO, which among all eukaryotic phytoplankton exhibits the lowest affinities for its substrate CO_2 (Morse et al., 1995, Badger et al., 1998). However several studies have indicated that ocean acidification alone had rather small effects on dinoflagellates (Rost et al., 2006; Eberlein et al., 2014). In dinoflagellate species *Scrippsiella trochoidea* and *Alexandrium tamarense* growth, elemental ratios and gross photosynthesis were not strongly affected under different CO_2 concentrations (Eberlein et al., 2014), suggesting that dinoflagellates are not carbon limited under current ocean conditions and have rather effective CCMs. However, the effects of ocean acidification on the

eco-physiology of microalgae might be strongly modulated when performing experiments with multiple stressors, such as temperature, light and nutrient availability. Several studies that combine ocean acidification with other factors have shown a strong modulation of CO_2 sensitivity, which affected phytoplankton eco-physiology (Fu et al., 2007; Gao et al., 2012; Li et al., 2012; Li & Campbell, 2013; Rokitta & Rost, 2012). As shown in **fig. 4**, alterations in oceanic CO_2 uptake will not be the only factor with severe changes on a short timescale due to anthropogenic activities.

Nitrogen limitation

Due to future warming and freshening of the ocean surface layers, increased seasonal stratification will be promoted in coastal regions and increased permanent stratification in the open ocean gyres (Hallegraeff, 2010; Fu et al., 2012). Phytoplankton relying on vertical mixing and nutrient input from below may be strongly affected, as during periods of enhanced upper ocean stratification NPP has been shown to decrease (Behrenfeld et al., 2006). Furthermore, with regard to ocean acidification, a lowering of the pH can inhibit nitrification. This could lead to a shift in N availability, for instance to more ammonium and organic N in the overall oceanic N inventory as compared to nitrate (Beman et al., 2011). Several physiological changes are to be expected when phytoplankton species are exposed to both CO_2 elevation and nutrient limitation. After carbon, nitrogen is among the most required nutrients for phytoplankton and it is often the limiting factor for primary production in the open ocean as well as in coastal regions (Tyrrell, 1999; Smayda, 1997; Elser et al., 2007). Additionally the assimilation pathways of C and N are very closely coupled (**fig. 5**) (Flynn, 1991; Turpin et al., 1991). Inorganic N is assimilated into amino acids via the glutamine synthetase/glutamate synthase (GS/GOGAT) cycle. The backbone needed for the amino acid synthesis is provided via the tricarboxylic acid cycle (TCA), which itself is supplied with phosphoglyceric acid (PGA) assimilated from CO_2. In addition, both assimilation processes have a high energy demand and compete for reductive equivalence in the cell. In view of elevated CO_2 concentrations in a nitrate-depleted future ocean, changes in C assimilation could strongly interact with N assimilation and lead to major eco-physiological shifts of the cells. For instance, the excess of energy from a down-regulation of the CCM could potentially be reallocated into N assimilation and thereby alter the nitrogen use efficiency (NUE). The NUE can be linked to the cellular C/N ratio, which indicates how much C has been incorporated per unit of N. Thus, an increase in cellular C/N ratio suggests an increase in NUE. Such an increase in NUE may not only cause an increase in population densities, but may also cause a further depletion of N. More specifically, an increase in NUE may lower the R* for N, which is the concentration of N where growth equals mortality. Species with a lower R* will be the superior competitor for that resource (Tilman 1982; Sterner & Elser, 2002). Thus, differential changes in R* by elevated pCO_2 may cause a shift in dominance of phytoplankton species. More specifically, some species might become better competitors under high CO_2 and low nutrient conditions as their R* decreases to lower values as compared to other species. In view of the predicted changes in inorganic C and N availability, responses in phytoplankton community composition are thus to be expected in the future ocean. Especially for

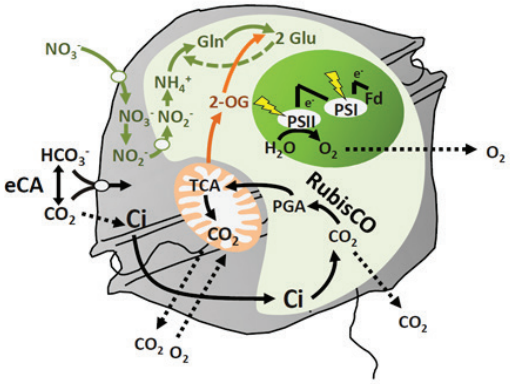

Figure 5. Schematic overview of C and N assimilation pathways in a phytoplankton cell

Schematic overview of the carbon (black) and nitrogen (green) assimilation pathways in a dinoflagellate cell. Represented here are respiration, photosynthesis, carbon acquisition via the CCM and N acquisition. The two pathways are coupled through the 2-oxoglutarate backbone (orange).

bloom-forming dinoflagellates, which tend to flourish late in phytoplankton succession when nutrients are generally depleted, research is crucial in order to understand the interactive effects of nutrient limitation and ocean acidification.

Working hypothesis

In this study the effects of elevated CO_2 concentrations in combination with N limitation will be determined for marine dinoflagellate species *Scrippsiella trochoidea* and *Alexandrium tamarense*, both isolated from the North Sea. *S. trochoidea* has the potential to form calcite cysts and is a cosmopolitan species that can form dense, non-toxic blooms, especially in stratified waters (Attaran-Fariman & Bolch, 2012). The genus *Alexandrium* is one of the major HAB-formers with regard to the diversity, magnitude and consequences of blooms (Anderson et al., 2012). Both species were grown under N limitation at different CO_2 levels in order to assess their response to these combined conditions. An increase in nitrate use efficiency is expected in response to elevated pCO_2, since C assimilation will have a lower energy demand and more energy could therefore be directed towards N assimilation. Furthermore, the toxicity of *A. tamarense* is expected to decrease in response to our experimental conditions due to the high N content of the toxins. For an accurate determination of combined effects of elevated CO_2 and N limitation, the dinoflagellates will be grown in newly developed continuous culture system, which have been shown to cause no mechanical stress on these two species (Van de Waal et al., 2014b). The advantage of such a system is that once growth rates of the cultures are limited by a single nutrient, the growth rate will eventually equal the dilution rate and a physiological steady-state in terms of nutrient concentration and biomass build-up is reached. Therefore we have a considerable amount of control on growth and resource concentration through the dilution rate compared to batch cultures. The period of resource limitation can also be extended over a longer period of time compared to batch culture approaches, where the period of resource limited growth is, depending on the growth conditions, generally short.

Material & Methods

Experimental conditions

The dinoflagellate species *S. trochoidea* GeoB267 (University of Bremen, Germany) and *A. tamarense* Alex5 (Tillmann et al., 2009), both isolates from the North Sea, were cultured at 15°C in 0.2 µm filtered North Sea water with a salinity of 34. The sea water was enriched with vitamins and trace metals according to the f/2 medium recipe (Guillard & Ryther, 1962) with additional H_2SeO_3 (10 nM) and $NiCl_2$ (6.27 nM) according to the recipe of K medium (Keller et al., 1987). Phosphate was added to a final concentration of 6.25 µM. The medium for *S. trochoidea* was not enriched with nitrate, having a concentration of around 8 µM. For *A. tamarense,* the medium was enriched with 8 µM nitrate yielding a final concentration of around 16 µM. Cultures were grown in specially designed glass tubes (370 mm length, 95 mm diameter) closed by a Duran GLS80 cap at both ends yielding a working volume of 2100 ± 50 mL. The glass tubes were positioned on a TL10 three-dimensional orbital shaker (Edmund Bühler GmbH, Hechingen, Germany), set at an angle of 9° with a shaking speed of 16 rpm, to allow gentle homogenous mixing (i.e. rocking) by means of a moving 55 mm diameter polyoximethylen (POM) ball and a 50-100 ml headspace (**fig. 6**; Van de Waal et al. 2014b). Light was provided from above by 18W/965 Biolux day light tubes (OSRAM GmbH, München, Germany) at a light-dark cycle of 16:8 h with an incoming PFD (photon flux density) of 250±30 µmol photons m^{-2} s^{-1} (Submersible Spherical Micro Quantum Sensor US-SQS/l, Heinz Walz GmbH, Germany). Medium was continuously supplied using a peristaltic pump and set to a dilution rate of 0.2 and 0.15 d^{-1} for *S. trochoidea* and *A. tamarense,* respectively. At the same rate, culture medium was flowing out of the continuous cultures through overpressure.

In order to obtain high CO_2 concentrations in seawater, cultures are usually directly aerated with high pCO_2. Dinoflagellates, however, are very vulnerable to turbulence (Thomas & Gibson 1990). Therefore the medium was pre-aerated in a tank, before it was pumped into the chemostat (**fig. 6**). The pre-aeration was performed using air containing 2000-3000 µatm pCO_2 into the tank. Elevation of pCO_2 can be omitted by mixing CO_2 free air (<0.1 µatm pCO_2; Domnick Hunter, Willich, Germany) with pure CO_2 (Air Liquide Deutschland, Düsseldorf, Germany) using mass flow controllers (CGM 2000 MCZ Umwelttechnik, Bad Nauheim, Germany). CO_2 concentrations were often verified by a dispersive infrared analyzer system (LI6252, LI-COR Biosciences, Bad Homburg, Germany). Tubes connecting the chemostat with the culture vessels were made of Tygon in order to prevent degassing of CO_2 from the high CO_2 pre-aerated medium. Due to biomass build-up, and losses by transport of the medium to the culture vessel, these initially extremely high CO_2 concentrations yielded reasonable future CO_2 concentrations predicted for the end of this century, i.e. 600 – 800 µatm (IPCC 2007). The ambient CO_2 treatment was obtained by equilibration of the medium with the atmosphere.

All treatments were performed in biological duplicates. Prior to experiments, cells were grown in a dilute batch ap-

proach for at least 5 generations. For the low and two high CO_2 experiments, cells were acclimated to 400 and 1000 µatm pCO_2, respectively. In continuous culture experiments with a fixed dilution rate (i.e. chemostat approach), cell densities reach a steady-state when cultures grow into resource limitation and growth rate eventually equals the dilution rate. In **fig. 7**, the development of biomass build-up and resource depletion of a modelled chemostat run are represented. For more details on the culturing method, see also Van de Waal et al. (2014b).

Sampling

Samples were taken daily or every other day, approximately 5-7h after the start of the light period, in order to determine population densities, carbonate chemistry and residual inorganic N concentrations. When cultures grew into nitrate limitation, cell densities and carbonate chemistry reached a steady-state, which was sampled over a period of at least three generations and seven days, with a medium exchange of 200% of the total volume in the chemostats. Subsequently the entire culture vessels were harvested to determine additional parameters, such as chlorophyll *a* content and elemental composition of the cells.

Population densities and growth rates

Population densities were determined

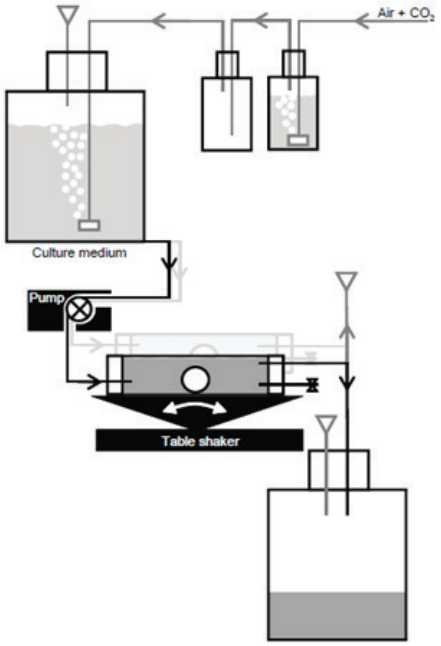

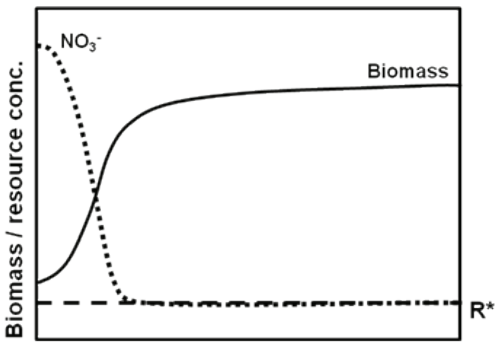

Figure 6. Schematic overview of the continuous culture set-up (left)

Shematic overview of the continuous culture set-up. Culture medium is pre-aerated in 10 L reservoirs with humidified air, containing different pCO_2. The pre-aerated medium is pumped into the chemostats at a fixed rate (i.e. dilution rate). Cultures are homogeneously mixed by gentle rocking of the orbital shaker, which moves a ball and headspace in opposite directions. Through overpressure, culture seawater flows out of the vessels and into the waste tank (picture from Van de Waal et al., 2014b).

Figure 7. The chemostat concept with nitrate as a limiting resource (right)

A schematic diagram of a chemostat run, showing biomass build-up, behaving according to Monod kinetics, and resource depletion (NO_3-) over time. The amount to which nitrate is depleted, when biomass build-up reached its maximum is called R* (dashed line).

using a coulter counter (Multisizer 3 coulter counter, Beckman Coulter GmbH, Germany), within a range of 10-60 µm of 1 ml sample. Additionally, samples were fixed with 1 % v/v iodine-potassium iodide solution (i.e. Lugol solution) and counted using an Axiovert 40C inverted microscope (Carl Zeiss MicroImaging GmbH, Hamburg, Germany). Population densities presented in this study were entirely based on microscopic cell counts, as this approach was found to be more reliable. Initial growth rates were subsequently determined at the start of the experiment, when the pump was still off, using an exponential fit function describing the change in population density through time:

$$N(t) = N(0)e^{\mu t}$$

where N(t) is the cell number, N(0) the initial cell number, µ the growth rate and t represents time in days. The cell surface was also measured with an inverted microscope, using the Axxiovert 200 M program. Please not that while the initial growth was likely not affected by NO_3^- availability, the growth during steady-state was fixed by the dilution rate.

Carbonate chemistry

The pH in the chemostates was determined with a three-point calibrated pH meter (826 pH mobile, Metrohm, Germany). For determination of DIC, a 2 x 4 ml sample of each culture was filtered through a 0.2 µm syringe filter (Nalgene, Denmark). Analysis of the DIC samples was performed in a QuAAtro high performance microflow analyzer (Seal, Mequon, USA) with a mean accuracy of 8 µmol kg^{-1}. Samples for TA analysis were taken at the point of inoculation and the end of each experiment. 200 ml of suspended culture was filtered through cellulose nitrate filters (0.2 µm, Whatman Freiburg, Germany) and analyzed by a fully automated titration system (TitroLine Alpha plus, Schott-Geräte GmbH, Meinz, Germany) with an average precision of 13 µmol kg^{-1}. pCO_2 was subsequently calculated based on pH_{NBS} (National Bureau of Standards) and DIC (**table 1**) using the CO_2sys program (Pierrot et al., 2006) with equilibrium constants of Mehrbach et al. (1973), refitted by Dickson and Millero (1987).

Nitrogen concentrations

N concentrations in the culture vessels were closely monitored by sampling

CO_2 treatment (µatm)	TA (µmol l^{-1})	DIC (µmol l^{-1})	pH_{NBS}	pCO_2 (µatm)
Scrippsiella trochoidea				
300	2353±26	2148±8.7	8.29±0.04	305±32
	2345±57	2149±4.4	8.31±0.03	291±23
600	2386±27	2224±14.4	8.03±0.02	615±25
	2393±17	2222±11.7	8.04±0.01	587±12
800	2365±11	2257±6.4	7.92±0.03	822±31
	2366±11	2246±6.1	7.96±0.04	764±29

Table 1. Carbonate chemistry for each biological replicate during steady-state

Carbonate chemistry for each biological replicate during steady-state. Values for DIC and pH indicate the mean value during steady-state [four days, three generations] (± SD). TA values represent the mean of t(0) and t(end) (n=2, ±SD). pCO_2 was calculated based on pH and DIC of each incubation, using the CO_2sys program (Pierrot et al., 2006) with equilibrium constants of Mehrbach et al. (1973), refitted by Dickson and Millero (1987).

every other day. 2 x 13 ml was sampled from the chemostats, filtered through a 0.2 µm syringe filter (Nalgene, Denmark) and stored in 15 ml acid-washed (overnight), milli-Q rinsed and with respective culture medium rinsed vials. Samples were directly placed at -20°C. Samples were analyzed with a nanomolar nutrient system (Ocean Optics Inc., USA). The system comprised of liquid waveguide capillary cells connected to a conventional segmented-flow auto-analyzer and using miniaturized spectrophotometers. The analysis of NO_3^- involves reduction of NO_3^- to NO_2^-, usually using a copperised cadmium column. Subsequently NO_2^- is determined spectrophotometrically (at 540 nm) following formation of a highly coloured dye through diazotisation with sulphanilamide and coupling with N-(1-naphthyl)-ethylenediamine dihydrochloride. Thereby the sum of the NO_3^- and NO_2^- concentrations is determined. In order to calculate the NO_3^- concentration, it is necessary to measure NO_2^- separately in the sample (by omitting the reduction step) and subtract it from the combined NO_2^- + NO_3^- measurement. For more details on this methods, see Patey et al. (2008).

Chlorophyll a

Chl *a* samples were taken at the end of each experiment. More specifically, 2 x 200 ml suspended culture was filtered through nitrate acetate filters (Whatman, Freiburg, Germany) and flash frozen in liquid nitrogen. Filters were subsequently stored at -80 °C until analysis. Extraction and determination of Chl *a* was done after Knap et al. (1996), using a TD-700 Fluorometer (Turner Designs, Sunnyvale, USA), and according to:

$$\text{Chl } a \ (\mu g\ L^{-1}) = \left(\frac{Fm}{Fm-1}\right)(F_0 - F_a)K_x\left(\frac{vol_{ex}}{vol_{filt}}\right)$$

where F_m is the acidification coefficient (F_0/F_a), F_0 is the reading before acidification, Fa is the reading after acidification, K_x is the steepness of the regression curve from the calibration calculations, volex is the extraction volume, and volfilt is the sample volume.

Elemental composition

The elemental composition of the cells, i.e. total particulate carbon (TPC), particulate organic carbon (POC), particulate inorganic carbon (PIC; difference between TPC and POC), and particulate organic nitrogen (PON), were determined with an Fison EA1108 elemental analyzer (Thermo Scientific, Waltham, USA). For this end, 2 x 200 ml suspended culture was filtered through pre-combusted (400°C, 5 h) GF/F filters (Whatman, Freiburg, Germany). The filters were subsequently placed in pre-combusted glass Petri dishes. For determination of POC, 200 µl of 0.1M HCl was added to the filters in order to remove inorganic carbon. All samples were dried overnight at 40°Cand stored at -20°C. Filters contained approximately 1.8 µmol N and 40 µmol C. The gas stream from the elemental analyzer was passed through a split interface, which injected a portion of the flow directly into the ion source of a Finnigan Delta-S mass spectrometer for the isotope ratio measurement. The isotopic composition for each sample was measured continuously as the C and N peaks from the elemental analyzer passed through the system (continuous-flow isotope ratio mass spectrometry). Each analysis was preceded by three injections of a working reference gas (ultra-high-purity N_2, $d^{15}N$= -8.09‰) and followed by a fourth injection to provide a highly accurate estimate of the difference in isotope ratios ($^{15}N/^{14}N$) and ($^{13}C/^{12}C$) between the sam-

ple and the reference gas. The ^{13}C and ^{15}N content of the samples were expressed as δ^{15}NPON and $\delta^{13}C_{POC}$:

$$\delta^{15}N_{PON}\ (‰) = \left[\frac{(^{15}N/^{14}N\ \text{sample})}{(^{15}N/^{14}N\ \text{atmosphere})} - 1\right] \times 1000$$

$$\delta^{13}C_{PON}\ (‰) = \left[\frac{(^{13}C/^{12}C\ \text{sample})}{(^{13}C/^{12}C\ \text{atmosphere})} - 1\right] \times 1000$$

For more details on the method, see Montoya et al. (1996).

Isotopic fractionation

In order to determine the isotopic composition of DIC ($\delta^{13}C_{DIC}$), 3x4 ml of each culture was filtered through a 0.2 µm syringe filter (Nalgene, Denmark) and stored at 3°C. Prior to analyses, 0.7 ml of sample was transferred to 8 ml vials. For determination of $\delta^{13}C_{DIC}$, the headspace was filled with helium and the sample was acidified with three drops of a 102% H_3PO_4 solution. The isotopic composition of CO_2 in the headspace was measured after equilibration using a GasBench-II coupled to a Thermo Delta-V advantage isotope ratio mass spectrometer with a precision of <0.1‰. The isotopic composition of CO_2 ($\delta^{13}C$-CO_2) was calculated from $\delta^{13}C_{DIC}$ using a mass balance relation according to Zeebe & Wolf-Gladrow (2001), applying fractionation factors between CO_2 and HCO_3^- from Mook et al. (1974) and between HCO_3^- and CO_3^{2-} from Zhang et al. (1995). Subsequently the isotopic fractionation during POC formation (p) was calculated relative to $\delta^{13}C_{CO2}$ according to Freeman and Hayes (1992):

$$\varepsilon_p = \frac{\delta^{13}C_{CO2} - \delta^{13}C_{POC}}{1 + \delta^{13}C_{POC} \times 10^{-3}}$$

For more details on this method, see also Van de Waal et al. (2013).

Toxin measurements

In order to analyze the cellular paralytic shellfish poisoning toxin (PST) content of *A. tamarense,* 200 ml culture of each chemostat was centrifuged for 15 min at 10,000 g and 4°C. The supernatant was transferred into an LC vial and analysed by liquid chromatography via fluorescence detection (LC-FD) with post-column derivatization (Krock et al., 2007). Different analogues of PSTs were analyzed and included the non-sulfated e neurotoxin saxitoxin (STX) and neosaxitoxin (NEO), the mono-sulfated gonyautoxins GTX1/4 and GTX2/3, and the di-sulfated C1/C2. The cellular toxicity was estimated based on the cellular PST content and the relative toxicity of each PST analogue (Wiese et al., 2010; Van de Waal et al., 2014a).

Results

The presented results are exclusively from *S. trochoidea,* as the data-set from *A. tamarense* is not completed yet. A preview of the results from the experiments with *A. tamarense* can be found in the appendix.

The development of a so-called physiological steady-state was reached after approximately 15 days, at which the reproductive rate of a culture equaled its mortality rate imposed by dilution and the supply rate of nutrients is balanced its consumption (**fig. 8**; **fig. 9**). Cultures were subsequently kept in steady-state for three more generations to extend the period of exposition to nitrate limitation.

Carbonate chemistry

The pCO_2 in the chemostats was followed over the course of the experi-

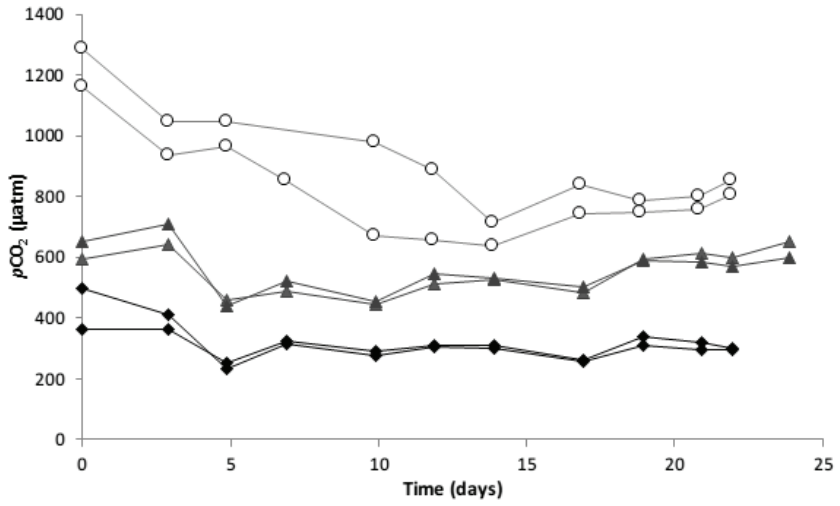

Figure 8. Carbonate chemistry in the chemostats over time

pCO_2 over the course of the experiments for the three different CO_2 treatments in duplicates. White circles represent the 800 CO_2 treatments, grey triangles represent the 600 CO_2 treatments and black diamonds represent the 300 CO_2 treatments.

ments (20-25 days; **fig. 8**, **table 1**). Due to biomass build-up in the chemostats, the pCO_2 used for the aeration of medium in the reservoir was set at higher concentrations to yield a reasonably high pCO_2 in the chemostats (predicted in a future ocean). A steady-state in carbonate chemistry was reached in all cultures after a period of approximately 15 days, with significantly different pCO_2 concentrations between the three treatments. The treatments represent a pre-industrial scenario, with 298±27 µatm pCO_2, and two future scenarios with 601±24 and 793±42 µatm pCO_2, respectively. At the start of the experiments pCO_2 concentrations were higher, with 428±96, 624±40 and 1225±90 µatm pCO_2, respectively.

Population densities

Initial nitrate concentrations supported a higher growth rate as compared to the dilution rate, resulting in an increase in population densities from days 0 to 5. Once nitrate concentrations became limiting, a steady-state in population densities was reached around day 7. Experiments lasted for more than 20 days and **fig. 9**. shows the population densities of *S. trochoidea* for the three different CO_2 treatments during this time.

After a period of approximately 7 days, population densities reached a steady-state with only minor fluctuations in population densities thereafter. Even though cells were inoculated in the chemostat at the same density, the two lower CO_2 treatments reached a steady-state earlier than the highest CO_2 treatment, with higher initial growth rates (~0.55 compared to ~0.4). The 300 and the 800 CO_2 treatments reached a steady-state with similar population densities of 481±55 and 474±26 cells ml^{-1}, respectively. In the 600 CO_2 treatment, population density were significantly higher with 653±102 cells ml^{-1} (t-test, P = 0.0002).

Cell size and elemental composition

Cell size and elemental composition of the cultures were determined in the

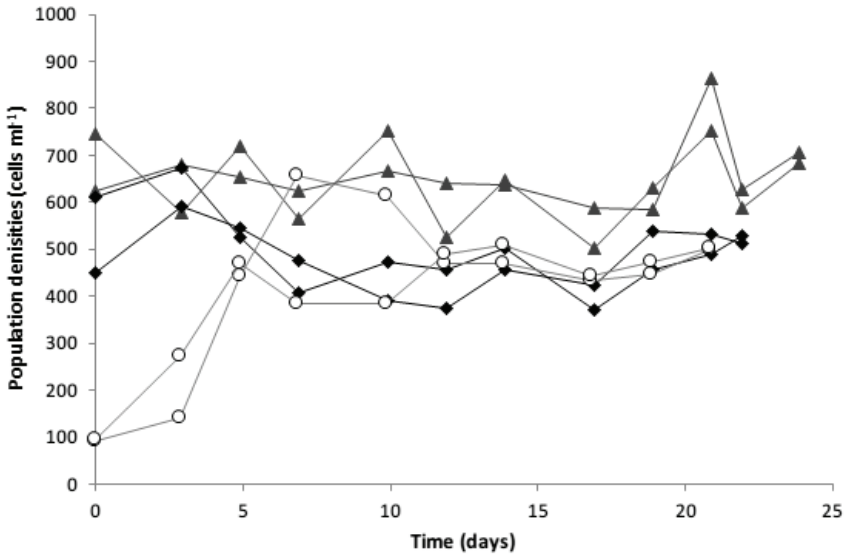

Figure 9. Population densities of *S. trochoidea* in the chemostats over time

Population densities of *S. trochoidea* against time for the three different CO_2 treatments (n=2). White circles represent the 800 CO_2 treatments, grey triangles represent the 600 CO_2 treatments and black diamonds represent the 300 CO_2 treatments.

steady-state covering at least 3 generations (**fig. 10**,**11**). In the different CO_2 treatments, POC and PON contents did not show much variations, with values varying between 3.86-4.37 and 0.19-0.27 ng cell^{-1}, respectively. The C/N ratios of *S. trochoidea* ranged between 18 and 25, being lowest in the high CO_2 treatment. Chl *a* content per cell as well as cell surface increased slightly over the applied pCO_2 range, both being highest in the 800 CO_2 treatment. In order to illustrate the effects of N limitation, results from this study were compared to the results from Eberlein et al. (2014, black symbols), which investigated the same strain of *S. trochoidea* under varying pCO_2 at N-replete conditions. For a comparison of both datasets, see discussion.

Residual nitrate

Once a steady-state was established for population densities and pCO_2, with nitrate as the limiting resource, the residual nitrate concentrations in the cultures were determined (**fig. 12**). The 300 and 600 CO_2 treatments yielded similar residual nitrate concentrations of 118±50 nmol l^{-1} and 126±46 nmol l^{-1}, respectively. While in the 800 CO_2 treatments, residual nitrate concentrations were higher with 348±138 nmol l^{-1}. A trend between the residual nitrate concentrations of the different CO_2 treatments could be observed, i.e. with increasing pCO_2, residual nitrate concentrations also became higher (polynominal fit with a R2 of 0.98, as a minimum to which cells can deplete N might be expected, see discussion; Tilman, 1982).

In order to assess whether R* is dependent on the NUE, the C/N ratios were plotted against residual nitrate concentrations (**fig. 13**). An inverse correlation could be observed, with a R^2 of 0.72 (linear regression, P = 0.032).

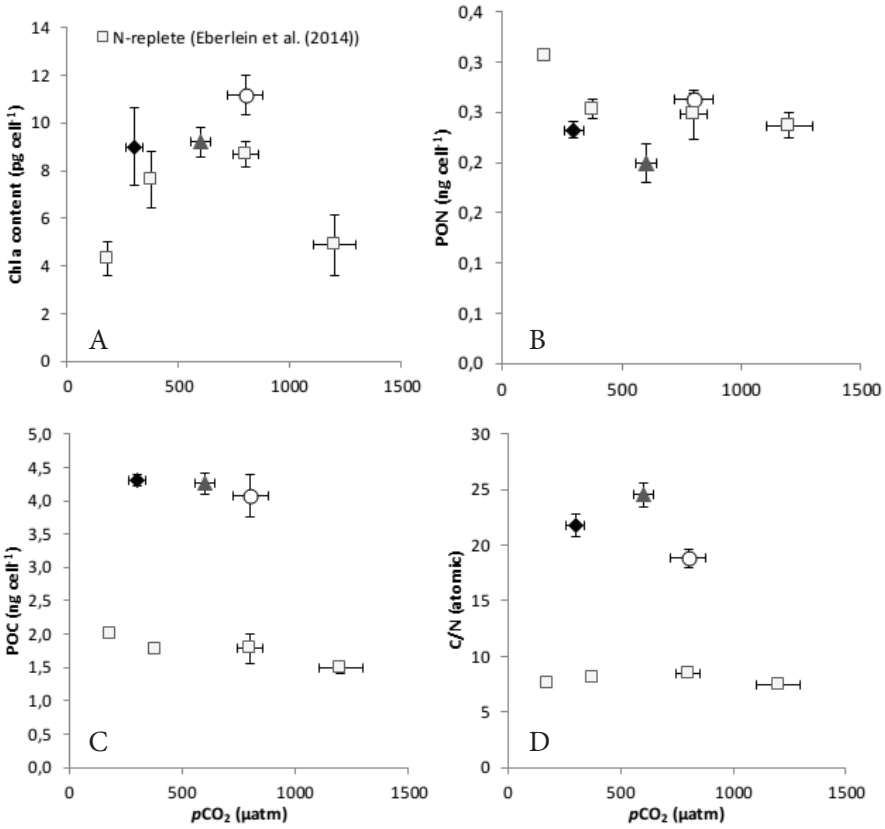

Figure 10. Chl *a* content (A), PON content (B), POC content against pCO_2 (C) and C/N ratio (D) as a function of pCO_2 for N-deplete and N-replete cultures

Chl *a* content as a function of pCO_2 (A). PON content as a function of pCO_2 (B). POC content as a function of pCO_2 (C). And the atomic C/N ratio as a function of pCO_2 (D). For the N-deplete conditions: black diamonds represent the 300 CO_2 treatment, grey triangles the 600 CO_2 treatment and white circles the 800 CO_2 treatment. the light grey squares represent N-replete conditions, derived from Eberlein et al. (2014).

Isotopic fractionation

$\delta^{13}C_{DIC}$ and $\delta^{13}C_{POC}$ were measured and isotopic fractionation (ε_p) was subsequently calculated for the different CO_2 treatments (**fig. 14**). POC was depleted in $\delta^{13}C$ relative to $\delta^{13}CO_2$ by about 9.2 to 12.1 ‰. A trend with increasing pCO_2 could not be recognized. ε_p does increase from 300 to 600 pCO_2 (linear regression, with a R2 of 0.94, P = 0.031), but due to relatively large differences among the biological replicates under 800 pCO_2, no further trend can be observed (linear regression, with a R^2 of 0.42, P = 0.36).

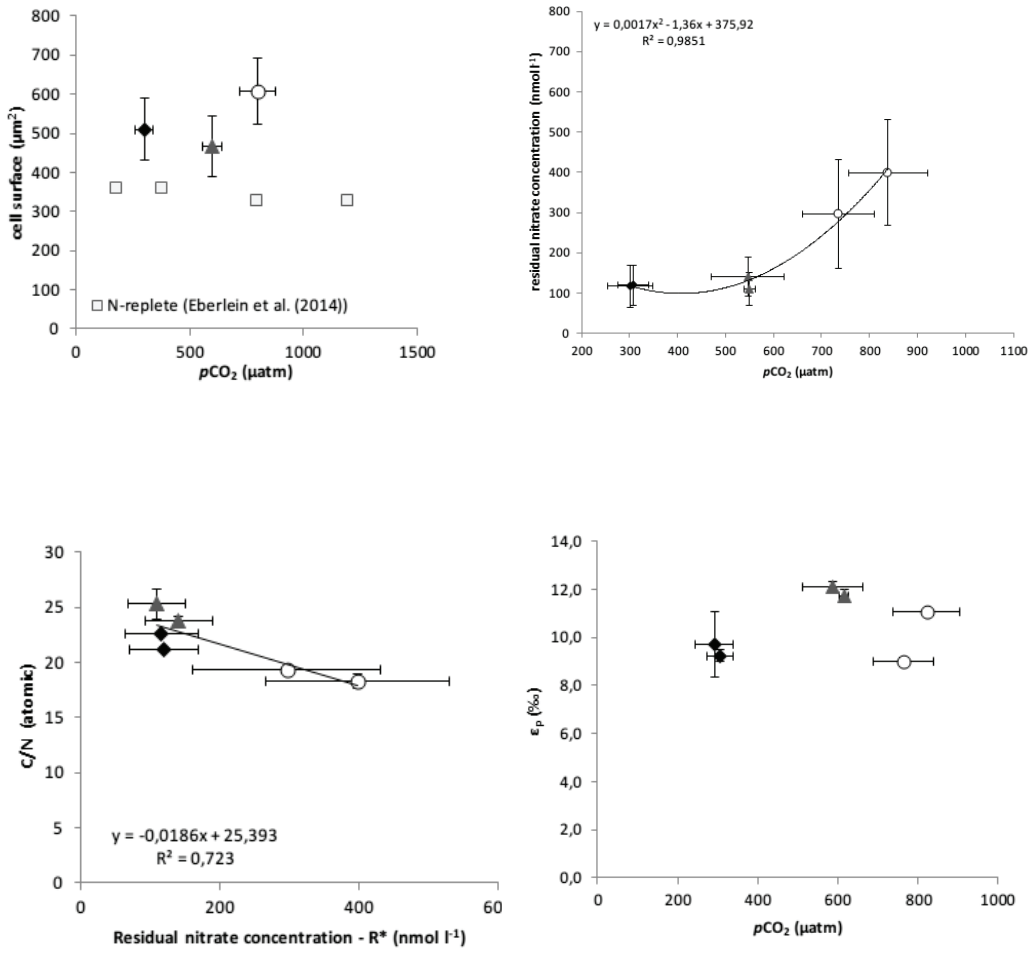

Figure 11. Cell surface of N-deplete and N-replete cultures over a range of pCO_2 (top left)

Cell surface against pCO_2 for *S. trochoidea* under N-deplete (a black diamond for the 300 CO_2 treatment, a grey triangle for the 600 CO_2 treatment and a white circle for the 800 CO_2 treatment) and N-replete (light grey squares) conditions. N-replete data was obtained from Eberlein et al. (2014).

Figure 12. Residual nitrate concentrations in the chemostats during steady-state (top right)

Residual nitrate concentrations against pCO_2 during physiological steady-state. White circles represent the 800 CO_2 treatments, grey triangles represent the 600 CO_2 treatments and black diamonds represent the 300 CO_2 treatments. The polynominal trend line emphasizes the relation between the treatments with a R^2 of 0.98 (equation represented in the graph).

Figure 13. C/N ratios against residual nitrate concentrations (bottom left)

White circles represent the 800 CO_2 treatments, grey triangles represent the 600 CO_2 treatments and black diamonds represent the 300 CO_2 treatments. The linear trend line emphasizes the relation between the treatments with a R^2 of 0.72 (equation represented in the graph).

Figure 14. Isotopic fractionation during POC formation (bottom right)

Isotopic fractionation during POC formation (ε_p) ‰ against pCO_2 µatm for *S. trochoidea*. White circles represent the 800 CO_2 treatments, grey triangles represent the 600 CO_2 treatments and black diamonds represent the 300 CO_2 treatments.

Discussion

In this study, the bloom-forming dinoflagellate *S. trochoidea* was exposed to different CO_2 concentrations in combination with N limitation, in order to determine the modulation of the effects of ocean acidification under nutrient limitation. Experiments were performed with a newly developed continuous culture system (Van de Waal et al. 2014b). While the elemental composition of *S. trochoidea* grown under N-deplete conditions did not show consistent changes in response to elevated pCO_2, the increase in the residual nitrate concentration suggested a shift in the resource use efficiency of *S. trochoidea*.

CO_2 effects under nitrogen limitation on dinoflagellates

Steady-state population densities were reached between 500 and 600 cells ml^{-1} in all chemostats, which are representative for naturally occurring populations of *S. trochoidea* (Morales-Blake et al., 2000). This is, however, not evident for chemostat experiments, as cultures are often grown into unrealistic high densities (Sciandra et al., 2003; Leornardos & Geider 2005; Bochard et al., 2011). Performing experiments with unnaturally high population densities can influence the response of the cultures to the experimental conditions, and most of all, it renders it impossible to test OA effects.

The elemental composition of *S. trochoidea* did not show an apparent response to CO_2 when grown under N-deplete conditions, and both the cellular POC and PON content remained largely unaltered over the applied CO_2 range, and responses were comparable to N-replete conditions (Eberlein et al., 2014). Chl *a* slightly increased with increasing CO_2 levels over the tested range, which is in accordance with the findings of Eberlein et al. (2014). Earlier studies have implicated dinoflagellates to be severely CO_2 limited due to their type II Rubisco and limited ability for HCO_3^- utilization (Colman et al., 2002; Dason et al., 2004). Thus, with increasing pCO_2 it is conceivable that growth and POC production will increase for this group of phytoplankton in particular. Recent studies, however, have shown that some dinoflagellate species are relatively independent from changes in CO_2 availability due to their possession of effective modes of CCMs (Rost et al., 2006; Ratti et al., 2007; Fu et al., 2008; Eberlein et al., 2014). Furthermore, the dinoflagellates Heterosigma akashiwo and Prorocentrum minimum were shown to have high HCO_3^- uptake rates (Fu et al., 2008), and *S. trochoidea* was also found to have a high HCO_3^- uptake (Eberlein et al., 2014). A preference for a certain carbon source can also be derived from the isotopic fractionation of POC, as HCO_3^- is enriched in ^{13}C relative to CO_2 (Rost et al., 2006). The observed ε_p values around 10‰, therefore also indicate *S. trochoidea* used both HCO_3^- and CO_2 as a carbon source, with predominantly HCO_3^- (Rost et al., 2006).

A down-regulation of the CCM in response to elevated pCO_2, as has been shown in other phytoplankton species such as diatoms and coccolithophores (Trimborn, 2009; Rokitta & Rost, 2012) is thus very likely to also occur in dinoflagellates. For instance, Rost et al. (2006) and Ratti et al. (2007) have shown a lowering of photosynthetic affinities for CO_2 and DIC in response to elevated pCO_2, and Van de Waal et al. (2013) observed

a down-regulation of CA transcripts at high pCO_2. A potential down-regulation of the CCM of *S. trochoidea* in this study could influence the N assimilation pathway, as more energy might become available for other cellular processes.

Nitrogen limitation effects on the elemental composition

There were no strong alterations in the elemental composition of *S. trochoidea* in response to elevated pCO_2. Much stronger alterations were observed in response to N limitation, when comparing the N-deplete cultures with the N-replete cultures from Eberlein et al. (2014). Li et al. (2012) also observed N limitation had a greater effect on elemental stoichiometry than elevated pCO_2 in the diatom species Phaeodactylum tricornutum. Their results furthermore suggested that the combined effects of both factors could act synergistically on photosynthetic rates and elemental stoichiometry, with highest C/N ratios in N limited and high pCO_2 cultures. Apparently, for *S. trochoidea,* N limitation had a stronger relative effect on the cellular N content than elevated pCO_2 had on the cellular C content. This relatively small effect of pCO_2 may be a result of the effective mode of CCM, providing *S. trochoidea* with sufficient carbon at present-day CO_2 levels (Eberlein et al., 2014).

A direct comparison between the N-deplete *S. trochoidea* cultures from this study and the N-replete *S. trochoidea* cultures from Eberlein et al. (2014) could be made, since experimental conditions between the studies were very similar. However, growing cultures in a dilute batch with ample nutrients, caused maximum growth rates under the imposed culture conditions, while in a chemostat approach, the growth rate is set by the dilution rate (and resembled approximately 33% of the growth observed in the dilute batch experiments). In contrast to our expectations, the PON content remained largely unaltered under N limitation. Similarly, also the Chl *a* content of the cells did not change upon N limitation, which is in line with an unaltered PON content as Chl *a* contains several nitrogen atoms and is generally considered a N-rich compound. Because cultures were severely N limited, with nitrate concentrations as low as 110 nmol l^{-1} during steady-state, it was expected that both the PON and Chl *a* content would decrease. Litchman et al. (2002) also performed experiments with dinoflagellates under N limitation in semi-continuous cultures, with starting nitrate concentrations of 5 and 25 µmol l^{-1}. The dinoflagellate species Akashiwo sanguinea and Gymnodinium cf. instriatum both showed a decrease in Chl *a* content, cell size and growth rate, however PON contents were not measured here. Li et al. (2012) also showed a decline in cell size, Chl *a* content and growth rates and C/N ratios increased under N limitation for diatom species Phaeodactylum tricornutum. Increases in C/N ratio under N limitation are expected to be primarily caused by a decrease in PON content. For *S. trochoidea,* however, the 2.5 fold increase in C/N ratios observed in the N-deplete compared to the N-replete cultures was mainly attributed to the increase in POC content. In fact, POC contents more than doubled under N-limitation while PON contents were comparable or showed a relatively small decrease, depending on the applied pCO_2. This increase in POC content caused the C/N ratio of *S. trochoidea* to deviate strongly from the Redfield ratio (i.e. a C/N of 6.6) and indicates N limitation (Redfield, 1934; Redfield, 1958; Sterner and Elser 2002). The unaltered PON and Chl *a* content in the N-deplete

cultures indicates *S. trochoidea* does not downscale its N metabolism and can maintain its photosynthetic machinery. As a consequence, cells may also maintain their photosynthetic rates, causing an excess of cellular carbon which cannot be allocated to cell growth leading to an increased POC content.

Growth rates in this study were fixed by the dilution rate at 0.2 d^{-1}, which is about 33% of the maximum growth rates observed in the N-replete dilute batch (Eberlein et al., 2014). Even though the cellular POC content increased upon N limitation, the POC production rates decreased from 1.06 ng $cell^{-1}$ day^{-1} under N replete to around 0.82 ng $cell^{-1}$ day^{-1} under N limited conditions. Photosynthesis is thus most likely not much affected if growth is considered, but nonetheless rates of POC production were lowered. Still, the energy derived via photosynthesis is also needed for cell division, but as *S. trochoidea* in N-deplete conditions divides three times slower, carbon fixation might serve as a sink for the excess in photosynthetic reduction equivalents, despite the lowered POC production rates. The apparent increase in cell size under N limitation also implied that the cells stored more carbon in their reserves. Indeed, dinoflagellates are known to store large quantities of carbon in starch (up to 30% by cells dry weight) and in lipid granules within the cytoplasm (Loeblich, 1977; Seo & Fritz 2002). However, cell size and POC content per cell are only partially correlated and approximately 40% of the increase in POC content can be explained by the increase in cell size.

A fraction of the high POC contents could also be explained by transparent exopolymer particles (TEP) production and its retainment on filters, depending on the filtered volume. Different phytoplankton species are known to excrete carbohydrates as a result of cellular carbon overflow, for instance when low nutrient concentrations limit growth but not photosynthesis, which can lead up to 40% of photosynthetically fixed carbohydrates being released as exudates (Baines & Pace, 1991; Corzo et al., 2000; Engel, 2002). These phytoplankton exudates can accumulate and lead to the abiotic formation of TEP and dinoflagellate species, as used in this study, have also been shown to contribute to TEP production (Engel, 2002; Passow, 2002; Claquin et al., 2008). TEP production, however, was not assessed in this study and so it remains unclear to what extent the increased POC content can be attributed to intracellular carbon stores and extracellular TEP.

CO_2 and nitrogen limitation effects on the resource use efficiency

As mentioned before, the NUE of a species can be defined as the amount of C that is fixed per available amount of N (Sterner & Elser, 2002). This may be indicated by the C/N stoichiometry of a cell as well, where an increasing NUE will result in an increase in C/N ratios. In addition, an increase in NUE may also lead to a higher biomass production, and may deplete the dissolved inorganic N concentration to a lower level. Thus, a high NUE may lead to a lower R* for nitrate (**fig. 7**), i.e. it will lower the concentration where growth equals the dilution rate under the predefined growth conditions (Tilman, 1982). The inverse correlation between NUE and R* was confirmed for this study, where the lowest R* values corresponded to the highest C/N ratios, i.e. the highest NUE (**fig. 13**).

In our experiments, *S. trochoidea* cells were able to deplete nitrate concentrations from initially 8 µmol l^{-1} to ~100

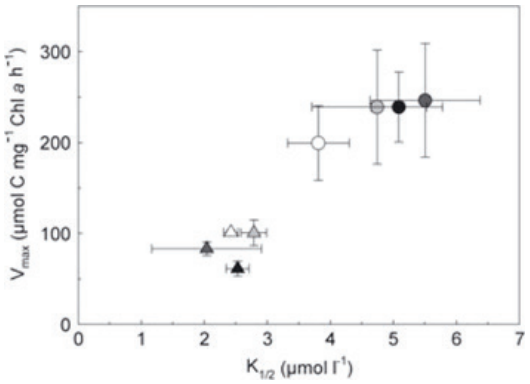

Figure 15. Vm against $K_{1/2}$ of photosynthetic carbon fixation

V_m against $K_{1/2}$ of photosynthetic carbon fixation for *S. trochoidea* (circles) and *A. tamarense* (triangles). The different colors in the symbols implicate the CO_2 treatment: white is 180 µatm, light grey is 380 µatm, dark grey is 800 µatm and black is 1400 µatm (Eberlein et al., 2014).

nmol l^{-1} in the two lowest CO_2 treatments. In the high CO_2 treatment, however, nitrate concentrations were depleted to 300-400 nmol l^{-1} (**fig. 10**). Even though residual nitrate concentrations between the 300 and the 600 CO_2 treatments were similar, *S. trochoidea* was able to increase biomass production in the 600 CO_2 treatment (yielding 600 cell ml^{-1} instead of 500 cell ml^{-1}), indicating the nitrate use efficiency of *S. trochoidea* increased over this CO_2 range. In the highest CO_2 treatment, however, biomass build-up was similar to the 300 CO_2 treatment, while residual nitrate concentrations were higher. Cells were thus not able to make use of the remaining nitrate and direct it towards biomass production, suggesting a decrease in NUE rather than an increase. The hypothesis that NUE would increase with elevated pCO_2 was based on the close coupling of the C and N assimilation pathways (**fig. 5**), and the competition for energy between both pathways. With elevated CO_2 levels, carbon assimilation may have a lower energy demand, since more CO_2 is taken up (through diffusion). An increase in diffusive CO_2 uptake under elevated pCO_2 was in fact shown for *S. trochoidea* (Eberlein et al., 2014). Therefore the excess of energy could be directed towards N assimilation, assuming the rate of photosynthesis in the different CO_2 treatments remains similar. Since photosynthetic rates were not measured in this study, it is not certain they remain unaltered in response to elevated pCO_2. However, the elemental composition of the cells, including Chl *a* quotas, did not show much variation in response to the different CO_2 treatments. This might indicate photosynthetic rates also remained largely unaltered over the applied CO_2 range.

According to the resource competition theory from Tilman (1982), Litchman et al. (2007) provided an equation which describes the dependency of the R*:

$$R^* = \frac{K_{1/2}}{V_{max}} \times Q_{min} \times m$$

where R* represents the nutrient competitive ability, $K_{1/2}$ the half-saturation constant, V_{max} the maximum uptake rate, Q_{min} the minimum internal nutrient concentration and m the mortality rate of a species. The ratio of V_{max} to $K_{1/2}$ is a commonly used measure of nutrient

acquisition capability, also called nutrient uptake affinity. A high affinity indicates a superior ability to acquire the specific nutrient (Healey 1980). Given the equation, an increase in affinity (a decrease in $K_{1/2}$ and/or an increase in V_{max}) or a decrease in Q_{min} and *m* would lower the R*. The affinity for photosynthetic carbon fixation of *S. trochoidea* was shown to decrease with increasing pCO_2 (**fig. 15**; Eberlein et al., 2014). Furthermore, a general trade-off within the kinetic properties of C acquisition has been observed, namely between the V_{max} and $K_{1/2}$ for carbon, based on biochemical constrains (Eberlein et al., 2014). A similar trade-off between V_{max} and $K_{1/2}$ was observed for nitrate acquisition in eukaryotic phytoplankton groups, including dinoflagellates (**fig. 16**; Litchman et al., 2007). Among the eukaryotic phytoplankton groups, dinoflagellates possess the lowest affinities for nitrate (Litchman et al., 2007). In the highest CO_2 treatment under N limitation, the observed increase in the residual nitrate concentrations suggests that affinities for nitrate uptake in *S. trochoidea* decreased even further. It is possible that the lower pH, as a consequence of elevated CO_2 levels, restrains the cell's nitrate uptake mechanism, as pH is suggested to affect the kinetics of nutrient uptake (Tilman et al., 1982; Button, 1985). The suggested inverse-bell shape of the trend line in **fig. 12** indicates *S. trochoidea* has an optimum for nitrate uptake (minimal residual nitrate concentrations, i.e. lowest R*) over the applied pCO_2 range (thus pH range). This optimum for nitrate uptake is also represented in the C/N ratio (**fig. 10**), which was highest in the 600 CO_2 treatment. Temperature may also affect R* according to an inverse-bell shaped pattern, with a clear optimum in competitive ability for different species (**fig. 17**; Tilman, 1999). In this study, the optimum pH range was most likely near the pH found in the 600 CO_2 treatment, as residual nitrate concentrations remained low while yielding a higher steady-state biomass as compared to the 300 µatm CO_2 treatment.

The observed increase in R* in the highest CO_2 treatment may also be explained by the increase in cell size, which negatively influences the NUE as the surface/volume ratio of the cell decreases. This decrease will either directly influence the NUE by a reduction in nitrate up-

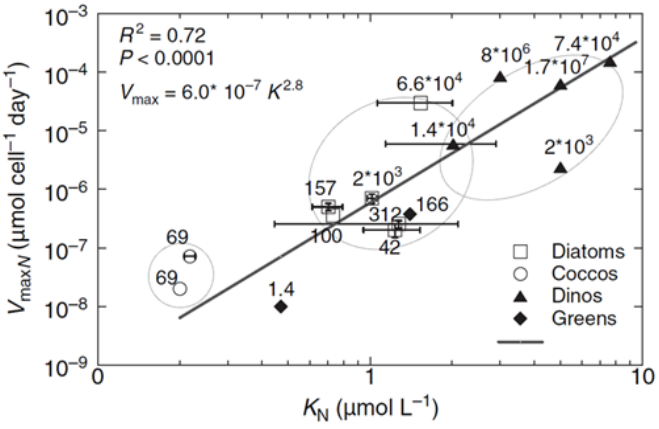

Figure 16. V_{max} against K_N of nitrate uptake

V_{maxN} in against K_N of nitrate uptake for the different eukaryotic phytoplankton groups. The solid line indicates a linear correlation between V_{maxN} and K_N (R^2=0.72, P<0.0001; Litchman et al., 2007).

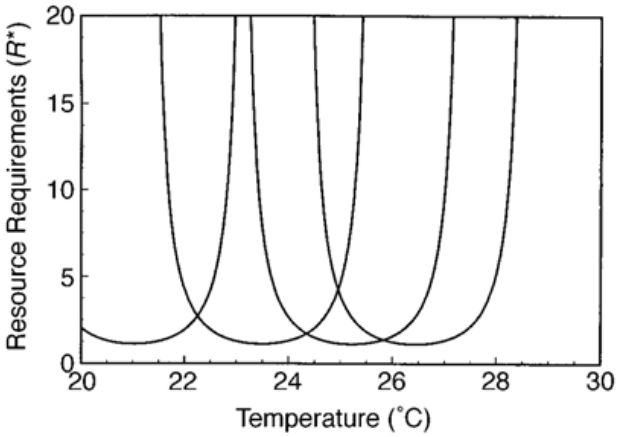

Figure 17. A model of resource competition in a habitat where temperature fluctuates

A model of resource competition in a habitat where temperature fluctuates, the resource requirements of the four species illustrated here (R*) depend on temperature, with each species having its maximal competitive ability (minimal R*) at a particular temperature (Tilman, 1999).

take or indirectly as C uptake may also become limited. However, the precise mechanisms behind the influence of different CO_2 concentrations on nitrate uptake remains to be elucidated in further experiments studying wider ranges of CO_2 availability.

Responses towards the combination of high CO_2 and nutrient limitation are most likely species-specific with different strategies behind the kinetics of their underlying physiology in order to optimize their competitive success. For instance, **fig. 15** also shows affinities for C fixation for the dinoflagellate species *A. tamarense*. The concurring low V_m and $K_{1/2}$ values for *A. tamarense* suggest it exhibits an 'affinity' strategy, with a competitive advantage under low carbon availability (Sommer 1984). Whereas *S. trochoidea* exhibits a 'velocity' strategy, with high V_{max} and $K_{1/2}$ values (Sommer, 1984), which suggests a competitive advantage under high and dynamic carbon availability. Trade-offs in these different strategies for adjusting assimilation pathways may allow species to coexist (Tilman, 1982; Hutchins et al., 2013; Eberlein et al., 2014)

Dinoflagellates in a future ocean

This study shows that elevated pCO_2 causes differential changes under N-deplete and N-replete conditions, and may reduce NUE of *S. trochoidea*. These shifts could eventually trigger changes in the dominance of species (Tilman et al., 1982). In other words, species benefiting from future scenarios (e.g. higher growth rates, lower R*) can possibly outcompete previously dominant species, which leads to alterations in the phytoplankton community composition. The decrease in R* observed for *S. trochoidea* would present a competitive disadvantage for this species and populations of *S. trochoidea* might decline when N availabilities are low (provided that other species, co-occurring with *S. trochoidea,* have a lower R*). Furthermore, a strong increase in C/N ratios was also observed under N limitation, which indicates the higher trophic levels of the food web will also be influenced in a future ocean as the nutritional value of primary producers will most likely decline (Van de Waal et al., 2010).

With respect to their underlying physi-

ology, dinoflagellates seem poor competitors as compared to other phytoplankton groups (Smayda, 1997). For instance, dinoflagellates possess the low-affine form II RubisCO (Morse et al., 1995), have the least affine nitrate uptake mechanism and exhibit low growth rates in comparison with other phytoplankton groups (Litchman et al., 2007). As they are an important component of the phytoplankton communities, however, they must have found means to thrive despite these physiological caveats.

Dinoflagellates make use of other strategies to persist in today's ocean. In contrast to other phytoplankton groups, dinoflagellate species with a completely autotrophic lifestyle are rare (Schnepf & Elbrächter, 1992). Most species lead a mixotrophic lifestyle, being able to photosynthesize, but also to ingest and digest food particles. Even though dinoflagellates are mostly mixotrophic, understanding their responses toward limitation of inorganic N is still important, since there are huge variations in photosynthetic and heterotrophic capabilities amongst dinoflagellate species (Jeong et al., 2010) and there may not always be food available. In addition, the vertical migratory behavior of dinoflagellates also allows them to persist, as they can easily migrate from the nutrient-rich deeper waters to the sunlit subsurface, where they also avoid grazing by zooplankton (Paerl & Scott, 2010). *A. tamarense* has been found in N-limited waters and is able to sustain growth and produce toxins by migrating to N-rich deeper ocean layers (MacIntyre et al., 1997). Under future ocean scenarios, traits involved in mixotrophy and migration may be particularly beneficial, since stratification and nutrient limitation likely become more pronounced (Paerl & Scott, 2010).

Dinoflagellates are also major causers of toxic HABs, and their toxicity is expected to be influenced by future pCO_2 and its consequences, although very little is still known (Fu et al., 2012). Van de Waal et al. (2014a) showed that PST content per cell as well as relative toxicity of *A. tamarense* decreased under elevated pCO_2. However, dinoflagellate species *Karlodinium veneficum* produced more toxic analogues of karlotoxins under elevated pCO_2 (Fu et al., 2010). Predictions for the future toxicity of HABs and for the ecological and economic consequences remain difficult, especially since toxin production and toxicity will additionally be influenced by changes in other resources, such as light and nutrients (Granéli & Flynn, 2006; Fu et al., 2012; Van de Waal et al., 2014a). For instance, karlotoxin productivity of *K. veneficum* increased under both P and N limitation (Adolf et al., 2009) and in *Dinophysis acuminate*, okadaic toxin productivity increased solely under N limitation (Johansson et al., 1996). In addition, the genus *Alexandrium* demonstrated increased toxicity under P limitation (Siu et al., 1997). PST content of *Alexandrium* will decline under N limitation, since these toxins are N-rich (Anderson et al., 1990; Flynn et al., 1994; Appendix). Furthermore the chemical speciation of nutrients can further alter algal toxicity, which is relevant with regard to ocean acidification, as a lowering of the pH is known to inhibit nitrification. This could lead to an increase in the concentration of reduced inorganic N species, such as ammonium, and on top of that, organic N is becoming more dominant in the overall oceanic N inventory than nitrate (Beman et al., 2011). Several bloom-forming dinoflagellates have proven to become more toxic when grown on reduced N species instead of nitrate, due to the difference in the costs of N assimilation (Fu et al.,

2012). Dinoflagellates will thus be greatly impacted by all the future changes in the oceans in relation to climate change, but eco-physiological responses will be very species-specific and shifts in species composition can therefore be expected.

Conclusions & Outlook

This study on the combined effects of elevated pCO_2 and N limitation on bloom-forming dinoflagellates showed that their eco-physiology was strongly affected. A change in NUE was observed for *S. trochoidea* in response to different levels of CO_2. Even though elevated pCO_2 did not show a strong effect on the elemental stoichiometry of the cells, provided that the areas and intensity of nutrient limitation are expanding, the alterations in phytoplankton cells due to N limitation will have a pronounced effect on the future ocean. The observed changes in elemental composition, i.e. higher POC content and C/N ratios, can have huge ecological consequences, for instance on the food web, as the nutritional value of the primary producers is already changing and will thus continue to be changed in the future. Alterations in N assimilation processes in our experiments are likely but remain unresolved since N uptake bio-assays and transcriptomic analyses were not performed in this study. It will, however, be of imperative importance to perform bio-assays in order to increase our understanding regarding the observed physiological changes and to assess phytoplankton responses to future ocean conditions (Rokitta & Rost, 2012; Van de Waal et al., 2013). In addition, this study emphasizes the importance of performing experiments using multiple stressors as CO_2 will not be the only changing parameter in the future oceans and effects of elevated CO_2 levels can be strongly modulated in combination with e.g. temperature, light and nutrient availability (Fu et al., 2007; Gao et al., 2012; Li et al., 2012; Li & Campbell, 2013; Rokitta & Rost, 2012). Multiple stressor experiments need to be performed using different phytoplankton species, as responses can be species- or even strain-specific (Fu et al., 2008; Brading et al., 2011). Furthermore, it would help to increase our understanding of the physiological processes taking place within the cell and to better predict the structure of future phytoplankton communities.

Appendix

A. tamarense population densities

Cultures of *A. tamarense* were grown at approximately 200 and 800 µatm pCO_2 in the chemostat during steady-state. Cultures in the low CO_2 treatment were kept in the chemostats for a period of 22 days, while the cultures of the high CO_2 treatment were kept in the chemostats longer than 35 days, since the biological duplicates did not reach a similar steady-state. **Fig. 18** shows the population densities of *A. tamarense* for the two different CO_2 treatments over time according to microscopic cell counts.

Population densities in the 300 CO_2 treatment reached a steady-state after approximately 10 days of ~550 cell ml^{-1} and were kept in a steady-state for another

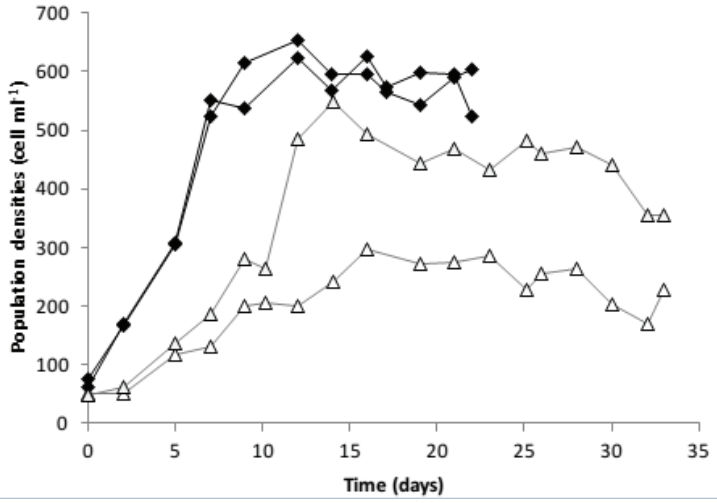

Figure 18. Time-course of *A. tamarense* in a chemostat under ambient pCO_2 (and N-depleted conditions)

Population densities of *A. tamarense* cells ml^{-1} against time days for the two different CO_2 acclimations in duplicates. The white triangles represent the 800 CO_2 acclimations and the black diamonds represent the 300 CO_2 acclimations.

10 days, which equals three generations. Population densities in the 800 CO_2 treatment had a lower initial growth rate than the low CO_2 acclimation and only one of the duplicates was able to reach cell densities of more than 400 cell ml^{-1} after ~15 days. The other high CO_2 duplicate was most likely unable to reach high cell densities because the volume within this chemostat was lower. As a result the dilution became higher and more cells were washed out of the chemostat. In the high CO_2 chemostats, the biological duplicates did not reach a similar steady-state and population densities started to decline after 25 days. An attempt to grow *A. tamarense* cultures at elevated pCO_2 again is currently in process.

A. tamarense toxin production

For the 300 CO_2 treatment toxins were already analyzed. The PST content per cell is represented in **fig. 19**. In order to emphasize the effects of N limitation on toxin production, results from this study were compared to the results from Van de Waal et al. (2014a), which investigated the same strain of *A. tamarense* (ALEX5) under N-replete conditions. Further experimental conditions between the studies were similar, except Van de Waal et al. (2014a) grew *A. tamarense* cultures in a dilute batch instead of chemostats and growth rates will therefore be different.

The total PST content of *A. tamarense* cells decreased as much as 85% under N limitation. This might be due to the N-richness of PSTs and due to the fact that amino acids form intermediates in toxin synthesis (Anderson et al., 1990; Flynn et al., 1994). This indicates an enormous decrease in cellular toxicity, although PST content does not solely determine cellular toxicity (Van de Waal et al., 2014a). The relative composition of the different PST analogues, with neurotoxin saxitoxin (STX), neosaxitoxin (NEO), gonyautoxins (GTX1, 2, 3 and 4), C1 and C2 as the most abundant ones, also determines the cellular toxicity (Van de Waal et al., 2014a). Therefore, also the PST composition was analyzed for *A. tamarense* and subsequently compared to the results from Van de Waal et al. (2014a; **fig. 20**). There are decreases in the STX and GTX2/3 analogues and

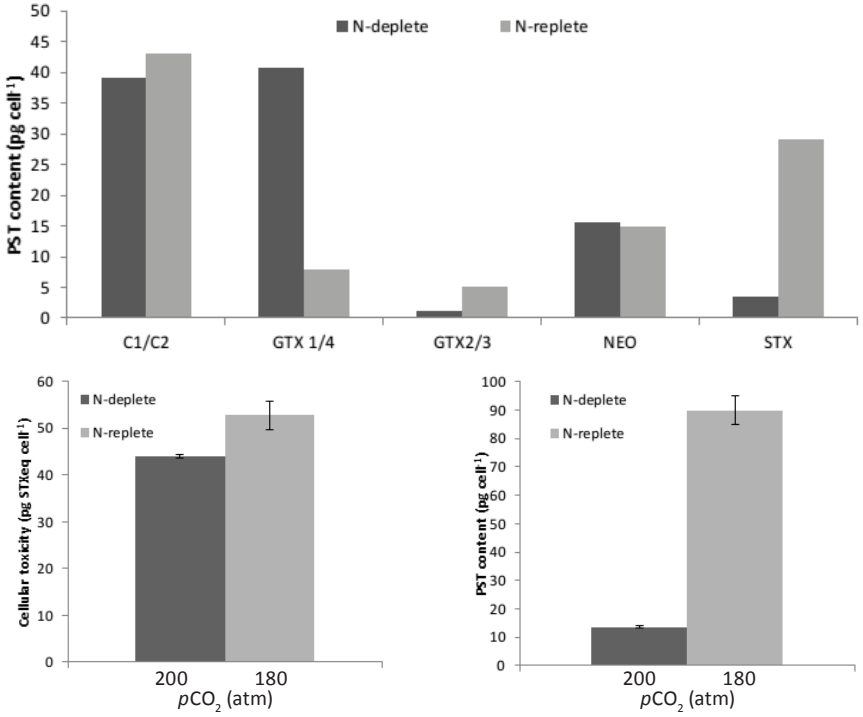

Figure 19. PST content of *A. tamarense* under N-replete and N-deplete conditions (bottom right)

PST content pg cell^{-1} for *A. tamarense* grown under N-replete (light grey) and N-deplete (dark grey) conditions. N-replete data was obtained from Van de Waal et al. (2014a).

Figure 20. Content of the different PST analogues under N-replete and N-deplete conditions (top)

Content of the different PST analogues (C1/C2, GTX1/4, GTX2/3, NEO and STX) ng cell^{-1} for *A. tamarense* under N-replete (light grey) and N-deplete (dark grey) conditions. N-replete data was obtained from Van de Waal et al. (2014a).

Figure 21. Cellular toxicity under N-replete and N-deplete conditions (bottom left)

Cellular toxicity pg STXeq cell^{-1} for *A. tamarense* grown under N-replete (light grey) and N-deplete (dark grey) conditions. N-replete data was obtained from Van de Waal et al. (2014a).

there is a considerable increase in the GTX1/4 analogues under N-deplete conditions. Non-sulfated analogues, such as STX and NEO are more toxic than the mono-sulfated analogues GTX1, 2, 3 and 4 or di-sulfated analogues C1 and C2. The observed shift from non-sulfated STX towards mono-sulfated GTX1/4 suggests that the relative toxicity decreased under N limitation. This is also proven by the cellular toxicity calculated based on the content and relative toxicity of each PST analogue (**fig. 21**; Wiese et al., 2010). Under future ocean conditions, the toxicity of *A. tamarense* is thus expected to decrease dramatically as PST content and relative toxicity both decrease under N limitation as well as under elevated pCO_2 (Van de Waal et al., 2014a).

Acknowledgements

I would especially like to thank Tim Eberlein for the opportunity to do this project with him and for introducing me to this interesting subject. I also thank him for the excellent supervision he provided throughout this whole project.

A special thanks also goes to Dr. Björn Rost and Dr. Dedmer van de Waal for their advice and guidance during the experimental phase of this project and for the constructive comments they provided for this thesis.

I thank Prof. Dr. Dieter Wolf-Gladrow for allowing me to do my Master project in his working group.

I also thank the whole biogeoscience section for the nice working environment I experienced during my stay in Bremerhaven.

Further I thank Prof. Dr. Eric Achterberg, Dr. Maren Voss, Dr. Uwe John, Nancy Kühne, Jana Hölscher for their involvement in this project and for the sample analyses.

I would like to thank Klaus-Uwe Richter and Ulrike Richter for working hard on the gas mixing system, so it could be used for our experiments.

A special thanks is also addressed to Dr. Francesca Sangiorgi, my supervisor at the University of Utrecht, who presented me with the opportunity to do my Master project at the AWI.

I would also like to thank Giulia Castellani for letting me stay at her house the last three months I was in Bremerhaven.

In addition I thank Tim van den Broek for designing the lay-out of this thesis.

Lastly I thank my family and friends for their support during my stay in Bremerhaven and during the time I was writing this thesis.

References

Adolf J.E., Bachvaroff T.R., Place A.R., Environmental modulation of karlotoxin levels in strains of the cosmopolitan dinoflagellate Karlodinium veneficum (Dinophyceae). (2009) J Phycol 45:176–192.

Anderson D.M., Kullis D.M., Sullivan J.J., Hall S., Lee C., Dynamics and physiology of saxitoxin production by dinoflagellates *Alexandrium* spp. (1990) Mar Biol 104:511-524

Anderson D.M., Glibert P.M., Burkholder J.M., Harmful algal blooms and eutrophication: Nutrient sources, composition, and consequences. (2002) Estuaries 25(4):704-726.

Anderson D.M., Alpermann T.J., Cembella A.D., Collos Y., Masseret E., Montresor M., The globally distributed genus *Alexandrium:* Multifaceted roles in marine ecosystems and impacts on human health. (2012) Harmful Algae 14:10-35.

Attaran-Fariman G., Bolch C.J.S., Morphology and phylogeny of *Scrippsiella trochoidea* (Dinophyceae) a potentially harmful bloom forming species isolated from the sediments of Iran's south coast. (2012)Iranian Journal of Fisheries Sciences 11: 252-270.

Badger M.R., Andrews T.J., Whitney S.M., Ludwig M., Yellowlees D.C., Leggat W., Price G.D., The diversity and coevolution of Rubisco, plastids, pyrenoids, and chloroplast-based CO_2-concentrating mechanisms in algae. (1998) Canadian Journal of Botany 76(6):1052-1071.

Baines S.B., Pace M.L., The production of dissolved organic matter by phytoplankton and its importance to bacteria: pattern across marine and fresh water systems. (1991) Limnology and Oceanography 36:1078-1090.

Behrenfeld M.J., O'Malley R.T., Siegel D.A., McClain C.R., Sarmiento J.L., Feldman G.C., Milligan A.J., Falkowski P.G., Letelier R.M., Boss E.S., Climate-driven trends in contemporary ocean productivity. (2006) Nature 444: 752-755.

Beman J.M., Chow C.E., King A.L., Feng Y., and others. Global declines in oceanic nitrification rates as a consequence of ocean acidification. (2011) Proc Natl Acad Sci USA 108:208–213.

Bochard C., Borger A.V., Handel N., Engel A., Biogeochemical response of Emiliania huxleyi (PML B92/11) to elevated pCO_2 and temperature under phosphorous limitation: A chemostat study. (2011) Journal of Experimental Marine Biology and Ecology 410:61-71.

Brading P., Warner M.E., Davey P., Smith D.J., Achterberg E.P., Suggett D.J., Differential effects of ocean acidification on growth and photosynthesis among phylotypes of Symbiodinium (Dinophyceae). (2011) Limnol Oceanogr 56:927–938.

Brading P., Warner M.E., Smith D.J., Suggett D.J., Contrasting modes of inorganic carbon acquisition amongst Symbiodinium (Dinophyceae) phylotypes. (2013) New Phytol 200:432–442.

Button D.K., Kinetics of Nutrient-Limited Transport and Microbial Growth. (1985) Microbiological reviews 49(3):270-297.

Cai W.J., Hu X., Huang W.J., Murrell M.C., and others. Acidification of subsurface coastal waters enhanced by eutrophication. (2011) National Geoscience 4:766-770.

Caldeira K., Wickett M.E., Anthropogenic carbon and ocean pH. (2003) Nature 425:365.

Capone D.G., Burns J.A., Montoya J.P., Subramanian A., Mahaffey C., Gunderson T., Michaels A.F., Carpenter E.J., Nitrogen fixation by Trichodesmium spp.: an important source of new nitrogen to the tropical and subtropical North Atlantic Ocean. (2005) Global Biogeochem Cycles 19, GB2024, doi: 10.1029/2004GB002331.

Claquin P., Probert I., Lefebvre S., Veron B., Effects of temperature on photosynthetic parameters and TEP production in eight species of marine microalgae. (2008) Aquatic Microbial Ecology 51:1-11.

Colman B., Huertes I.E., Bhatti S., Daron J.S., The diversity of inorganic carbon acquisition mechanisms in eukaryotic microalgae. Functional Plant Biology 29:261-270.

Corzo A., Morillo J.A., Rodríguez S., Production of transparent exopolymer particles (TEP) in cultures of Chaetoceros calcitrans under nitrogen limitation. (2000) Aquatic Microbial Ecology 23:63-72.

Crosson E.R., A cavity ring-down analyzer for measuring atmospheric levels of methane, carbon dioxide, and water vapor. (2008) Applied Physics B 92(3):403-408.

Dason J.S., Huertas I.E., Colman B., Source of inorganic carbon for photosynthesis in two marine

dinoflagellates. (2004) J Phycol 40:229–434.

Dickson A.G., An exact definition of total alkalinity and a procedure for the estimation of alkalinity and total inorganic carbon from titration data. (1981) Deep Sea Research Part A. Oceanographic Research Papers 28(6):609–623.

Dickson A.G., Millero F.J., A comparison of the equilibrium constants for the dissociation of carbonic acid in seawater media. (1987) Deep-Sea Res 34:1733–1743.

Doney S.C., Schimel D.S., Carbon and Climate System Coupling on Timescales from the Precambrian to the Anthropocene. (2007) Annual Review of Environment and Resources 32:31-66.

Doney S.C., Fabry V.J., Feely R.A., Kleypas J.A., Ocean Acidification: The Other CO_2 Problem. (2009) Annual Review of Marine Science 1:169-192.

Eberlein T., Van de Waal D.B., Rost B., Differential effects of ocean acidification on carbon acquisition in two bloom-forming dinoflagellate species. (2014) Physiologia Plantarum doi:10.1111/ppl.12137.

Elser J.J., Bracken M.E.S., Cleland E.E., Gruner D.S., Harpole W.S., Hillebrand H., Ngai J.T., Seabloom E.W., Shurin J.B., Smith J.E., Global analysis of nitrogen and phosphorus limitation of primary producers in freshwater, marine and terrestrial ecosystems. (2007) Ecology Letters 10:1–8.

Engel A., Direct relationship between CO_2 uptake and transparent exopolymer particles production in natural phytoplankton. (2002) Journal of Plankton Research 24(1):49-53.

Falkowski P.G., Katz M.E., Knoll A.H., Quigg A., Raven J.A., Schofield O., Taylor F.J.R., The Evolution of Modern Eukaryotic Phytoplankton. (2004) Science 305(5682):354-360.

Falkowski P.G., The role of phytoplankton photosynthesis in global biogeochemical cycles. (2004) Photosynthesis Research 39:235-258.

Falkowsky P.G., Raven J.A., Aquatic photosynthesis. (2007) Princeton University Press, Princeton, NJ

Falkowski P.G., Knoll A., Evolution of primary producers in the sea. (2007) Elsevier Academic Press, London, UK.

Field C.B., Behrenfeld M.J., Randerson J.T., Falkowski P., Primary production of the biosphere: integrating terrestrial and oceanic components. (1998) Science 281: 237–240.

Flynn K.J., Algal carbon-nitrogen metabolism: a biochemical basis for modelling the interactions between nitrate and ammonium uptake. (1991) Journal of Plankton Research 13(2): 373-387.

Flynn K., Franco J.M., Fernandez P., Reguera B., Zapata M., Wood G., Flynn K.J., Changes in toxin content, biomass and pigments of the dinoflagellate *Alexandrium* minutum during nitrogen refeeding and growth into nitrogen and phosphorous stress. (1994) Mar Ecol Prog Ser 111:99-109.

Forster P., Ramaswamy V., Artaxo P., Berntsen T., Betts R., Fahey D.W., Haywood J., Lean J., Lowe D.C., Myhre G., Nganga J., Prinn R., Raga G., Schulz M., Van Dorland R., Changes in Atmospheric Constituents and in Radiative Forcing" in Climate Change 2007: The Physical Science Basis: Contribution of Working Group I to the Fourth Assessment Report of the Intergovernmental Panel on Climate Change, eds. S. Solomon, D. Qin, M. Manning, et al. (2007) Cambridge University Press, Cambridge, United Kingdom and New York, NY, USA.

Freely R.A., Sabine C.L., Hernandez-Ayon J.M., Ianson D., Hales B., Evidence for upwelling of corrosive 'acified' water onto the continental shelf. (2008) Science 320:1490-1492.

Freeman H.J., Hayes J.M., Fractionation of carbon isotopes by phytoplankton and estimates of ancient CO_2 levels. (1992) Global Biogeochem Cycles 6:185–198.

Fu F.X., Warne M.E., Zhang Y., Feng Y., Hutchins D.A., Effects of increased temperature and CO_2 on photosynthesis, growth, and elemental ratios in marine Synechococcus and Prochlorcoccus (Cyanobacteria). (2007) Journal of Phycology 43:485–496.

Fu F.X., Zhang Y., Warner M.E., Feng Y., Sun J., Hutchins D.A., A comparison of future increased CO_2 and temperature effects on sympatric Heterosigma akashiwo and Prorocentrum minimum. (2008) Harmful Algae 7:76–90.

Fu F.X., Place A.R., Garcia N.S., Hutchins D.A., CO_2 and phosphate availability control the toxicity of the harmful bloom dinoflagellate Karlodinium veneficum. (2010) Aquat Microb Ecol 59:55-65.

Fu F.X., Tatters A.O., Hutchins D.A., Global change and the future of harmful algal blooms in the ocean. (2012). Mar Ecol Prog Ser 470:207–233.

Gao K., Xu J., Gao G., Li Y., Hutchins D.A., Huang

B., Wang L., Zheng Y., Jin P., Cai X., Häder D., Li W., Xu K., Liu N., Riebesell U., Rising CO_2 and increased light exposure synergistically reduce marine primary productivity. (2012) Nature Climate Change 2:519–523.

Garrison T., Oceanography: an invitation to marine science. (2007) Thomson Brooks/Cole, Belmont, CA, USA.

Glibert P., Seitzinger S., Heil C.A., Burkholder J.M., Parrow M.W., Codispoti L.A., Kelly V., The role of eutrophication in the coastal proliferation of harmful algal blooms: new perspectives and new approaches. (2005) Oceanography 18:198–209.

Giordano M., Beardall J., Raven J.A., CO_2 concentrating mechanisms in algae: mechanisms, environmental modulation, and evolution. (2005) Annu. Rev. Plant Biol 56:99–131.

Granéli E., Flynn K., Chemical and physical factors influencing toxin content, in: E. Granéli, J.T. Turner (Eds.), Ecology of harmful algae. (2006) Springer-Verlag Berlin Heidelberg, Heidelberg: 229-241.

Guillard R.R.L., Ryther J.H., Studies of marine planktonic diatoms: I. Cyclotella nana hustedt, and Detonula confervacea (cleve) gran. (1962) Canadian Journal of Microbiology 8(2):229-239.

Hallegraeff G.M., Ocean climate change, phytoplankton community responses, and harmful algal blooms: a formidable predictive challenge. (2010) J Phycol 46:220–235.

Healey F.P., Physiological indicators of nutrient deficiency in lake phytoplankton. . (1980) Can. J. Fish Aquat Sci 37:442–453.

Hoegh-Guldberg O., Mumby P.J., Hooten A.J., Steneck R.S., Greenfield P., Gomez E., Harvell C.D., Sale P.F., Edwards A.J., Caldeira K., Knowlton N., Eakin C.M., Iglesias-Prieto R., Muthiga N., Bradbury R.H., Dubi A., Hatziolos M.E., Coral reefs under rapid climate change and ocean acidification. (2007) Science 318(5857):1737-1742.

Hoppenrath M., Saldarriaga J.F., Dinoflagellates. Version 15 December 2012. (2012) http://tolweb.org/Dinoflagellates/2445/2012.12.15.

Houghton J.T., Ding Y., Griggs D.J., Nouger M., van der Linden P.J., Dai X., Maskell K., Johnson C.A., Climate change 2001: the scientific basis. Contribution of working group I to the 3rd assessment report of the Intergovernmental Panel on Climate Change. (2001) Cambridge University Press, United Kingdom.

Hutchins D.A., Fei-Xue F., Webb EA, Walworth N, Tagliabue A. Taxon-specific response of marine nitrogen fixers to elevated carbon dioxide concentrations. (2013)Nat Geosci 6: 790–795.

Intergovernmental Panel on Climate Change. Working group I report: The physical science basis. (2007) available at: http://ipcc-wg1.ucar.edu/wg1/wg1-report.html.

Jansen E., Overpeck J., Briffa K.R., Duplessy J.C., Joos F., Masson-Delmotte V., Olago D., Otto-Bliesner B., Peltier W.R., Rahmstorf S., Ramesh R., Raynaud D., Rind D., Solomina O., Villalba R., Zhang D., "Palaeoclimate" in Climate Change 2007: The physical science basis: contribution of working group I to the fourth assessment report of the Intergovernmental Panel on Climate Change, eds. S. Solomon, D. Qin, M. Manning, et al. (2007) Cambridge University Press, Cambridge, and New York, NY, USA.

Jeong H.J., Yoo Y.D., Kim J.S., Seong K.A., Kang N.S., Kim T.H., Growth, feeding and ecological roles of the mixotrophic and heterotrophic dinoflagellates in marine planktonic food webs. Ocean Science Journal 45(2):65-91.

Jiao N., Herndl G.J., Hansell D.A., Benner R., Kattner G., Wilhelm S.W., Kirchman D.L., Weinbauer M.G., Luo T., Chen F., Azam F., Microbial production of recalcitrant dissolved organic matter: long-term carbon storage in the global ocean. (2010) Nature Reviews Microbiology 8:593-599.

Johansson N., Graneli E., Yasumoto T., Carlsson P., Legrand C., Toxin production by Dinophysis acuminata and D. acuta cells grown under nutrient sufficient and deficient conditions. In: Yasumoto T, Oshima Y, Fukuyo Y (eds) Harmful and toxic algal blooms. (1996) Intergovernmental Oceanographic Commission of UNESCO, Paris, 277–280.

Jones P.D., Mann M.E., Climate over past millennia. (2004) Reviews of Geophysics 42, RG2002,-doi:10.1029/2003RG000143.

Karl D., Letelier R., Tupas L., Dore J., Christian J., Hebel D., The role of nitrogen fixation in biogeochemical cycling in the subtropical North Pacific Ocean. (1997) Nature 388:533-538.

Keeling R.F., Piper S.C., Bollenbacher A.F., Walker J.S., Atmospheric carbon dioxide record from Mauna Loa. (2005) http://cdiac.ornl.gov/trends/co2/sio-mlo.html.

Keller M.D., Selvin R.C., Claus W., Guillard R.R.L., Medium for the culture of oceanic ult-

raphytoplankton. (1987) Journal of Phycology 23(4):633–638.

Krock B., Seguel C.G., Cembella A.D., Toxin profile of *Alexandrium* catenella from the Chilean coast as determined by liquid chromatography with fluorescence detection and liquid chromatography coupled with tandem mass spectrometry. (2007) Harmful Algae 6(5):734-744.

Leonardos N., Geider, R.J., Elevated atmospheric carbon dioxide increases organic carbon fixation by Emiliania huxleyi (Haptophyta), under nutrient-limited high-light conditions. (2005) Journal of Phycology 41:1196-1203.

Li W., Gao K., Beardall J., Interactive effects of ocean acidification and nitrogen limitation on the diatom Phaedactylum tricornutum. PLoS ONE 7(12):e51590

Li G., Campbell D.A., Rising CO_2 interacts with growth light and growth rate to alter photosystem II photo inactivation of the coastal diatom Thalassiosira pseudonana. (2013) PLoS ONE 8:e55562.

Litchman E., Neale P.J., Banaszak A.T., Increased sensitivity to ultraviolet radiation in nitrogen-limited dinoflagellates: Photoprotection and repair. (2002) Limnol. Oceanogr 47(1):86–94.

Litchman E., Klausmeier C.A., Schofield O.M., Falkowski P.G., The role of functional traits and trade-offs in structuring phytoplankton communities: scaling from cellular to ecosystem level. (2007) Ecology Letters 10:1170–1181.

Loeblich A.R. III, Studies on synchronously dividing populations of Cachonina niei, a marine dinoflagellate. (1977) Bulletin of Japanese Society of Phycology 25, supplement (Memorial Issue of Dr. Yamada): 119-128.

Lüthi D., Le Floch M., Bereiter B., Blunier T., Barnola J., Siegenthaler U., Raynaud D., Jouzel J., Fischer H., Kawamura K., Stocker T. F., High-resolution carbon dioxide concentration record 650,000–800,000 years before present. (2008) Nature 453:379–382.

MacIntyre J.G., Cullen J.J., Cembella A.D., Vertical migration, nutrition and toxicity in the dinoflagellate *Alexandrium tamarense*. (1997) Mar Ecol Prog Ser 148:201–216.

Maier-Reimer E., Mikolajewicz U., Winguth A., Future ocean uptake of CO_2: interaction between ocean circulation and biology. (1996) Climate Dynamics 12(10):711–722.

Mehrbach C., Culberson C.H., Hawley J.E., Pytkowicz R.M., Measurement of the apparent dissociation constants of carbonic acid in seawater at atmospheric pressure. (1973) Limnol Oceanogr 18:897–907.

Mook W.G., Bommerso J.C., Staverma W.H., Carbon isotope fractionation between dissolved bicarbonate and gaseous carbon-dioxide. (1974) Earth and Planetary Science Letters 22:169–176.

Morales-Blake A., Hernández-Becerril D., Cavazos-Guerra C. Registros de Mareas Rojas en las Bahías de Manzanillo, Colima, México. In: Estudios sobre plancton en México y el Caribe. (2000) E. Ríos-Jara, E. Juárez-Carrillo, M. Pérez-Peña. (eds.) Sociedad Mexicana de Planctología y Universidad de Guadalajara 81-82.

Morse D., Salois P., Markovic P., Woodland Hastings J., A nuclear-encoded form II RubisCO in Dinoflagellates. (1995) Science 268: 1622-1624.

Nelson D.M., Treguer P., Brzezinski M.A., Leynaert A., Queguiner B., Production and dissolution of biogenic silica in the ocean: revised global estimates, comparison with regional data and relationship to biogenic sedimentation. (1995) Global Biogeochemical Cycles 9:359–359.

Olli K., Anderson D.M., High encystment success of the dinoflagellate Scrippsiella cf. lachrymosa in culture experiments. (2002) Journal of Phycology 38(1):145-156.

Paerl H.W., Scott J.T., Throwing fuel on the fire: synergistic effects of excessive nitrogen inputs and global climate change on harmful algal blooms. (2010) Environ Sci Technol 44:7756–7758.

Passow U., Transparent exopolymer particles (TEP) in aquatic environments. (2002) Progress in Oceanography 55:287-333.

Patey M.D., Rijkenberg M.J.A., Statham P.J., Stinchcombe M.C., Achterberg E.P., Mowlem M., Determination of nitrate and phosphate in seawater at nanomolar concentrations. (2008) Trends in Analytical Chemistry 27(2):169-182.

Pearson P.N., Palmer M.R., Atmospheric carbon dioxide concentrations over the past 60 million years. (2000) Nature 406:695–699.

Petit J.R., Jouzel J., Raynaud D., Barkov N.I., Barnola J.M., Basile I., Bender M., Chappellaz J., Davis M., Delaygue G., Delmotte M., Kotlyakov V.M., Legrand M., Lipenkov V.Y., Lorius C., Pepin L., Ritz C., Saltzman E., Stievenard M., Climate and atmospheric history of the past 420 000 years from the Vostok ice core, Antarctica. (1999) Nature 399:429–436.

Pierrot D.E., Lewis E., Wallace D.W.R., Program developed for CO_2 system calculations. Carbon dioxide information analysis center, Oak Ridge National Laboratory. (2006) Available at: http://cdiac.ornl.gov/oceans/co2rprt.html.

Post W.M., Peng T., Emanuel W.R., King A.W., Dale V.H., DeAngelis D.L., The global carbon cycle. (1990) American Scientist 78: 310-326.

Ratti S., Giordano M., Morse D., CO_2-concentrating mechanisms of the potentially toxic dinoflagellate Protoceratium reticulatum (Dinophyceae, Gonyaulacales). (2007) Journal of Phycology, doi: 10.1111/j.1529-8817.2007.00368.x.

Raven J.A., Beardall J., Carbon acquisition mechanisms of algae: carbon dioxide diffusion and carbon dioxide concentrating mechanisms. (2003) Photosynthesis in algae , eds. S.E. Douglas, A.W.D. Larkum & J.A. Raven, Springer:225-244.

Raven J., Caldeira K., Elderfield H., Hoegh-Guldberg O., Liss P., Riebesell U., Shepherd J., Turley C., Watson A., Ocean acidification due to increasing atmospheric carbon dioxide. (2005) The Clyvedon Press Ltd, Cardiff, UK.

Redfield A.C., On the proportions of organic derivations in sea water and their relation to the composition of plankton. (1934) In James Johnstone Memorial Volume. (ed. R.J. Daniel). University Press of Liverpool 177–192.

Redfield A.C., The biological control of chemical factors in the environment (1958) American Scientist.

Rokitta S.D., Rost B., Effects of CO_2 and their modulation by light in the life-cycle stages of the coccolithophore Emiliania huxleyi. (2012) Limnology & Oceanography 57(2):607-618.

Rost B., Riebesell U., Burkhardt S., Sültemeyer D., Carbon acquisition of bloom-forming marine phytoplankton. (2003) Limnol Oceanogr 48:55–67.

Rost B., Riebesell U., Coccolithophores and the biological pump: responses to environmental changes. In: Thierstein HR, Young JR (eds) Coccolithophores: from molecular processes to global impact. (2004) Springer Berlin, 99–125.

Rost B., Richter K., Riebesell U., Hansen P.J., Inorganic carbon acquisition in red tide dinoflagellates. (2006) Plant Cell Environ 29:810–822.

Rost B., Zondervan I., Wolf-Gladrow D.A., Sensitivity of phytoplankton to future changes in ocean carbonate chemistry: current knowledge, contradictions and research directions. (2008) Mar Ecol Prog Ser 373:227-237.

Riebesell U., Effects of CO_2 enrichment on marine phytoplankton. (2004) Journal of Oceanography 60(4):719-729.

Ruddiman W.F., Earth's climate past and future. (2008) W.H. Freeman and company, New York.

Sabine C.L., Feely R.A., Gruber N., Key R.M., Lee K., Bullister J.L., Wanninkhof R., Wong C.S., Wallace D.W.R., Tilbrook B., Millero F.J., Peng T., Kozyr A., Ono T., Rios A.F., The Oceanic Sink for Anthropogenic CO_2. (2004) Science 305(5682):367-371.

Sarmiento J.L., Murnane R., Le Quere C., Keeling R., Williams R.G., Air-Sea CO_2 Transfer and the Carbon Budget of the North Atlantic. (1995) Philosophical Transactions: Biological Sciences 348(1324):211–219.

Sarmiento J.L., Slater R., Barber R., Bopp L., Doney S.C., Hirst A.C., Kleypas J., Matear R., Mikolajewicz U., Monfray P., Soldatov V., Spall S.A., Stouffer R., Response of ocean ecosystems to climate warming. (2004) Global Biogeochemical Cycles 18, GB3003, doi: 10.1029/2003GB002134.

Schnepf E., Elbrächter M., Nutritional strategies in dinoflagellates. A review with emphasis on cell biological aspects. (1992) European Journal of Protistology 28(1):3-24.

Sciandra A., Harlay J., Lefevre D., Lemee R., Rimmelin P., Denis M., Gattuso J., Response of coccolithophorid Emiliania huxleyi to elevated partial pressure of CO_2 under nitrogen limitation. (2003) Mar Ecol Prog Ser 261:111-122.

Seo K.S., Fritz L., Diel changes in pyrenoid and starch reserves in dinoflagellates. (2002) Phycologia 41(I):22-28.

Siu G., Young M., Chan D., Environmental and nutritional factors which regulate population dynamics and toxin production in the dinoflagellate *Alexandrium* catenella. (1997) Hydrobiologia 352:117–140.

Smayda T.J., Harmful algal blooms: their ecophysiology and general relevance to phytoplankton blooms in the sea. (1997) Limnology and Oceanography 42(5):1137-1153.

Smith C.R., De Leo F.C., Bernardino A.F., Sweetman A.K., Arbizu P.M., Abyssal food limitation, ecosystem structure and climate change. (2008) Trends in Ecology and Evolution 23(9):518–528.

Solomon S., Qin D., Manning M., Climate Change 2007- the physical science basis: contri-

bution of working group I to the fourth assessment report of the Intergovernmental Panel on Climate Change. (2007) Cambridge University Press, United Kingdom.

Sommer U., The paradox of the plankton: fluctuations of phosphorus availability maintain diversity of phytoplankton in flow-through cultures. (1984) Limnol Oceanogr 29:633–636.

Sterner R.W., Elser J.J., Ecological Stoichiometry: The Biology of Elements from Molecules to the Biosphere. (2002) by Princeton University Press, US.

Sumich J.L., Morrissey J.F., Introduction to the biology of marine life. (2004) Jones & Bartlett Learning.

Suttle C.A., Viruses in the sea. (2005) Nature 437:356-361.

Thomas W.H., Gibson C.H., Effects of small-scale turbulence on microalgae. (1990) Journal of Applied Phycology 2(1):71-77.

Tilman, D., Resource Competition and Community Structure. (1982)Princeton University Press, Princeton, NJ.

Tilman D., Kilham S.S., Kilham P., Phytoplankton community ecology: the role of limiting nutrients. (1982) Ann Rev Ecol Syst 13:349-372.

Tilman D., The ecological consequences of changes in biodiversity: a search for general principles. (1999) Ecology 80(5):1455–1474.

Tillmann U., Alpermann T.L., da Purificacao R.C., Intra-population clonal variability in allelochemical potency of the toxigenic dinoflagellate *Alexandrium tamarense*. (2009) Harmful Algae 8:759–769.

Tortell P.D., Morel F.M.M., Sources of inorganic carbon for phytoplankton in the eastern subtropical and equatorial Pacific Ocean. (2002) Limnol Oceanogr 47:1012–1022.

Trimborn S., Langer G., Rost B., Effect of calcium concentration and irradiance on calcification and photosynthesis in the coccolithophore Emiliania huxleyi. (2007) Limnol Oceanogr 52:2285–2293.

Trimborn S., Wolf-Gladrow D., Richter K., Rost B., The effect of pCO_2 on carbon acquisition and intracellular assimilation in four marine diatoms. (2009) Journal of Experimental Marine Biology and Ecology 376(1):26–36.

Turpin D.H., Effects of inorganic N availability on algal photosynthesis and carbon metabolism. (1991) Phycology 27:14-20.

Tyrrell T., The relative influences of nitrogen and phosphorus on oceanic primary production. (1999) Nature 400:525-531.

Van de Waal D.B., Verschoor A.M., Verspagen J.M.H., Van Donk E., Huisman J., Climate-driven changes in the ecological stoichiometry of aquatic ecosystems. (2010) Frontiers in Ecology and the Environment 8(3):145-152.

Van de Waal D.B., John U., Ziveri P., Reichart G., Hoins M., Sluijs A., Rost B., Ocean acidification reduces growth and calcification in a marine dinoflagellate. (2013) PLoS ONE 8:e65987

Van de Waal D.B., Eberlein T., John U., Wohlrab S., Rost B., Impact of elevated pCO_2 on paralytic shellfish poisoning toxin content and composition in *Alexandrium tamarense*. (2014a) Toxicon 78:58–67.

Van de Waal D.B., Eberlein T., Bublitz Y., John U., Rost B., Shake it easy: a gentle mixed continuous culture system for dinoflagellates. (2014b) J Plankton Res 0(0):1–6, doi:10.1093/plankt/fbt138.

Wang Z.H., Qi Y.Z., Yang Y.F., Cyst formation: an important mechanism for the termination of *Scrippsiella trochoidea* (Dinophyceae) bloom. (2007) Journal of plankton research 29(2):209-218.

Wiese M., D'Agostino P.M., Mihali T.K., Moffitt M.C., Neilan B.A., Neurotoxicalkaloids: Saxitoxin and its analogs. (2010) Mar Drugs 8:2185–2211.

Wilhelm S.W., Suttle C.A., Viruses and nutrient cycles in the sea. (1999) BioScience 49: 781-788.

Wolf-Gladrow D.A., Riebesell U., Burkhardt S., Bijma J., Direct effects of CO_2 concentration on growth and isotopic composition of marine plankton. (1999) Tellus B 51:461-476.

Wolf-Gladrow D.A., Zeebe R.E., Klaas C., Körtzinger A., Dickson A.G., Total alkalinity: The explicit conservative expression and its application to biogeochemical processes. (2007) Marine Chemistry 106:287-300.

Zeebe R.E., Wolf-Gladrow D.A., CO_2 in seawater: equilibrium, kinetics, isotopes. (2001) Elsevier Science, Amsterdam.

Zhang J., Quay P.D., Wilbur D.O., Carbon isotope fractionation during gaswater exchange and dissolution of CO_2. (1995)Geochimica Et Cosmochimica Acta 59:107–114.